Aalto University, School of Science and Technology
Applied Electronics Unit, Series B
Espoo, Finland, 2011 Research Reports B20

DETECTION OF HUMAN MOVEMENT BY NEAR FIELD IMAGING: DEVELOPMENT OF A NOVEL METHOD AND APPLICATIONS

Henry Rimminen

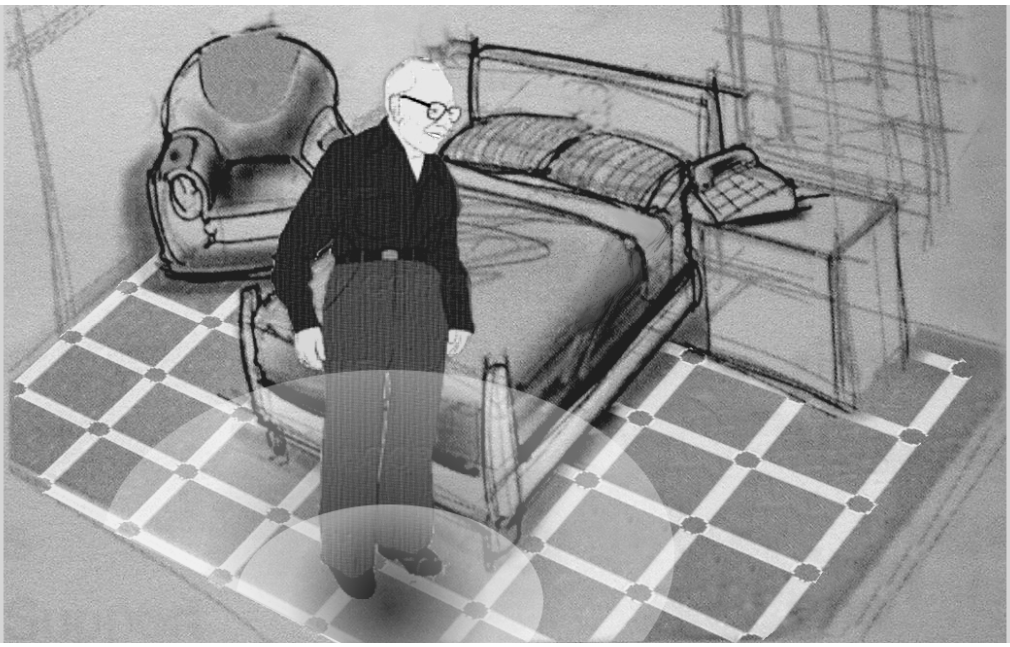

Aalto University
School of Science
and Technology

Applied Electronics Unit
School of Science and Technology
Aalto University
Espoo, Finland

DETECTION OF HUMAN MOVEMENT BY NEAR FIELD IMAGING: DEVELOPMENT OF A NOVEL METHOD AND APPLICATIONS

Henry Rimminen

Dissertation for the degree of Doctor of Science in Technology
to be presented with due permission of
the School of Science and Technology
for public examination and debate
in Auditorium S1 at Aalto University (Espoo, Finland)
on the 21st of January, 2011, at 12 noon.

Aalto University, School of Science and Technology, Applied Electronics Unit,
Series B, Research Reports B20
Espoo, Finland, 2011

Distribution:
Aalto University School of Science and Technology
Applied Electronics Unit
P.O. Box 13340
FI-00076 AALTO

ISBN 978-952-60-3496-6 (paper)
ISBN 978-952-60-3497-3 (electronic)
ISSN 1456-1174 (paper)
ISSN 1459-1111 (electronic)

Multiprint Oy
Espoo 2011

Aalto University

ABSTRACT OF DOCTORAL DISSERTATION	AALTO UNIVERSITY SCHOOL OF SCIENCE AND TECHNOLOGY P.O. BOX 11000, FI-00076 AALTO http://www.aalto.fi

Author Henry Rimminen

Name of the dissertation
Detection of Human Movement by Near Field Imaging: Development of a Novel Method and Applications

Manuscript submitted 24.9.2010	Manuscript revised 13.11.2010
Date of the defence 21.1.2011	
☐ Monograph	☒ Article dissertation (summary + original articles)

Faculty Faculty of Electronics, Communications and Automation
Department Department of Electronics
Field of research Applied Electronics
Opponent(s) Docent Jaakko Valvanne and Docent Timo Jämsä
Supervisor Professor Raimo Sepponen
Instructor Professor Raimo Sepponen

Abstract

The proportion of senior citizens is increasing, which requires more resources in the care services. The effectiveness of these services is proposed to be increased by remote monitoring of senior citizens living at home or in nursing homes. The monitoring can be performed with various types of sensors, but the solution presented here incorporates most of the functionalities found in related work in one comprehensive system.

The system that was developed uses electric field sensing to detect human presence and movement. Falls and the vital functions of a fallen person can also be extracted from the signals. The sensor arrangement consists of a matrix of thin planar electrodes under the floor surface, which makes the system completely undetectable and discreet. It is not disturbed by shading or darkness and does not require a lot of computing power. Computer vision does not enjoy these advantages. Furthermore, no devices need to be worn and no batteries need to be charged, as with systems based on transponders worn by the subject. If identification is required, the system developed in this work does not rule out the use of transponders.

The impedances of the electrodes are measured using a tuned transformer and a phase-sensitive detector. A signal-to-noise ratio of 37 dB has been achieved with this structure. The mean positioning error when observing people who are walking is 21 cm. Multiple people can be discriminated with a 90% certainty if the distance between them is 78 cm. The sensitivity and specificity in fall detection have been found to be 91% and 91%, respectively. The cardiac activity and respiration are clearly visible when a person lies prone or supine on the floor. A capacitive radio frequency identification (RFID) tag in a shoe was developed for person identification.

The system developed here has been installed in a large nursing home. The nurses have indicated their satisfaction in a comprehensive questionnaire, which was conducted by a representative of the nurses. Positive feedback has also been obtained from a senior person living alone and from his family members.

Keywords Electric field sensing, Near field imaging, Indoor tracking, Fall detection

ISBN (printed) 978-952-60-3496-6	ISSN (printed) 1456-1174
ISBN (pdf) 978-952-60-3497-3	ISSN (pdf) 1459-1111
Language English	Number of pages 70 p. + app. 50 p.

Publisher Aalto University, Faculty of Electronics, Communications and Automation

Print distribution Aalto University School of Science and technology, Applied Electronics Unit

☒ The dissertation can be read at http://lib.tkk.fi/Diss/2011/isbn9789526034973

Aalto-yliopisto

VÄITÖSKIRJAN TIIVISTELMÄ	AALTO-YLIOPISTO TEKNILLINEN KORKEAKOULU PL 11000, 00076 AALTO http://www.aalto.fi

Tekijä Henry Rimminen

Väitöskirjan nimi
Henkilön liikkeen havainnointi käyttämällä lähikenttäkuvantamista: uuden menetelmän kehitys ja sovellukset

Käsikirjoituksen päivämäärä 24.9.2010	Korjatun käsikirjoituksen päivämäärä 13.11.2010
Väitöstilaisuuden ajankohta 21.1.2011	
☐ Monografia	☒ Yhdistelmäväitöskirja (yhteenveto + erillisartikkelit)

Tiedekunta	Elektroniikan, tietoliikenteen ja automaation tiedekunta
Laitos	Elektroniikan laitos
Tutkimusala	Sovellettu Elektroniikka
Vastaväittäjä(t)	Dos. Jaakko Valvanne, Dos. Timo Jämsä
Työn valvoja	Prof. Raimo Sepponen
Työn ohjaaja	Prof. Raimo Sepponen

Tiivistelmä
Ikääntyneiden osuus väestöstä kasvaa, mikä luo tarpeen lisäresursseille hoivapalveluissa. Palveluiden tehokkuutta ehdotetaan lisättäväksi käyttämällä kehittyneitä valvontamenetelmiä yksinasuvien vanhusten kotona ja vanhainkodeissa. Valvonta voidaan toteuttaa monilla menetelmillä, mutta kehitetty menetelmä sisällyttää useimpien menetelmien edut yhteen kokonaisvaltaiseen järjestelmään.

Kehitetty järjestelmä käyttää sähkökenttiä ihmisten läsnäolon ja liikkeen tunnistamiseen. Myös kaatuminen ja kaatuneen elintoiminnot voidaan havaita. Anturijärjestelyyn kuuluu matriisi, joka koostuu ohuista elektrodeista lattiapinnan alla. Tämä tekee järjestelmästä huomaamattoman eikä se häiritse yksityisyyttä. Menetelmä ei häiriinny pimeydestä eikä siinä esiinny sokeita kohtia. Se ei myöskään vaadi paljoa tietojenkäsittelytehoa. Nämä seikat ovat tietokonenäön ongelmia.
Kannettavia laitteita ei tarvita, mikä poistaa paristojen lataamisen. Jos identifiointia vaaditaan, kehitetty järjestelmä ei sulje pois kannettavan transponderin käyttöä.

Elektrodien impedanssi mitataan käyttämällä viritettyä muuntajaa ja vaiheherkkää ilmaisinta. 37 desibelin signaali-kohina- suhde saavutettiin tällä rakenteella. Keskimääräinen paikannusvirhe on 21 cm ja monen kohteen erottelu onnistuu 90 % varmuudella, jos henkilöiden välimatka on 78 cm. Herkkyys ja spesifisyys kaatumisen tunnistuksessa on 91 % ja 91 %. Sydämen toiminta ja hengitys on havaittavissa, jos henkilö makaa vatsallaan tai selällään. Henkilön identifiointia varten kehitettiin kenkään asennettava kapasitiivinen RFID tagi (radio frequency identification).

Kehitetty järjestelmä on asennettu suureen vanhainkotiin. Järjestelmää käyttävät hoitajat ovat ilmaisseet tyytyväisyytensä kattavassa kyselytutkimuksessa, jonka teetti hoitajien edustaja. Positiivista palautetta on myös saatu yksinasuvalta vanhukselta ja hänen omaisiltaan.

Asiasanat sähkökenttämittaus, lähikenttäkuvantaminen, sisäpaikannus, kaatumisen havainnointi

ISBN (painettu)	978-952-60-3496-6	ISSN (painettu)	1456-1174
ISBN (pdf)	978-952-60-3497-3	ISSN (pdf)	1459-1111
Kieli	Englanti	Sivumäärä	70 s. + liit. 50 s.

Julkaisija Aalto-yliopisto, Elektroniikan, tietoliikenteen ja automaation tiedekunta

Painetun väitöskirjan jakelu Aalto-yliopiston teknillinen korkeakoulu, Sovelletun elektroniikan yksikkö

☒ Luettavissa verkossa osoitteessa http://lib.tkk.fi/Diss/2011/isbn9789526034973

Preface

This work was carried out at the Department of Electronics, School of Science and Technology, Aalto University during years 2006-2011. I am most grateful to the head of department, Professor Raimo Sepponen, for his leadership during the past years. I also thank him for guiding and for supervising this thesis. I consider him my mentor.

I am most grateful to our Laboratory Manager, Matti Linnavuo, for his co-authorship and his guidance in becoming an author. I also owe thanks to my colleagues for their support and encouragement.

Special thanks belong to Juha Lindström for co-authorship and for ideas concerning the embedded software.

Many thanks also belong to the staff of building 'A' at Kustaankartano for their patience in tuning the system and in the clinical tests. I also thank Harriet Finne-Soveri for her vision and confidence in us, which enabled us to pilot the system in a real environment.

I am grateful to the official pre-examiners of this thesis, Professors Timo Jämsä and Pertti Silventoinen, for their constructive comments.

Last but certainly not least, I would like to thank Tittamaria, who has supported me throughout the work and my son Noa Elias, who has brought sunshine into my life.

This study has been supported by Jenny and Antti Wihuri Foundation, European Union, the Graduate School, Faculty of Electronics, Communications and Automation and the Finnish Society of Electronics Engineers.

Henry Rimminen
Espoo, 2011

Contents

List of publications

This thesis consists of a summary and publications I to V

I H. Rimminen, M. Linnavuo, and R. Sepponen, "Human tracking using near field imaging," in *Proc. Second International Conference on Pervasive Computing Technologies for Healthcare,* Tampere, Finland, Jan. 30-Feb. 1, 2008, pp. 148-151.

II H. Rimminen and R. Sepponen, "Biosignals with a floor sensor," in *Proc. Second International Conference on Biomedical Electronics and Devices,* Porto, Portugal, Jan. 14-18, 2009, pp. 125-130.

III H. Rimminen, J. Lindström, and R. Sepponen, "Positioning Accuracy And Multi-Target Separation With A Human Tracking System Using Near Field Imaging," *International Journal on Smart Sensing and Intelligent Systems*, vol. 2, no. 1, Mar. 2009, pp. 156-175.

IV H. Rimminen, J. Lindström, M. Linnavuo, and R. Sepponen, "Detection of Falls Among the Elderly by a Floor Sensor Using the Electric Near Field," *IEEE Transactions on Information Technology in BioMedicine*, vol. 14, no. 6, Nov. 2010, pp. 1475 – 1476.

V H. Rimminen, M. Linnavuo, and R. Sepponen, "Human identification and localization using active capacitive RFID tags and an electric field floor sensor," *International Review of Electrical Engineering*, vol. 5, no. 3, Jun. 2010, pp. 1061-1068.

Author's contribution

Author's contribution to the publications

This chapter describes the author's contribution to the publications I – V. The co-authors have seen and approved the descriptions in this chapter.

Publication I presents the basic method for detecting a human presence with an electric field floor sensor and characterizes the measurement electronics. The author was the corresponding author. The tests to characterize the system and a human phantom were designed by the author. The circuits used in the system were designed and implemented by the author.

Publication II presents a method for recording the vital functions of a person lying on the sensor floor. The author was the corresponding author and he designed the test arrangement and the methods used to characterize and analyze the signals.

Publication III presents methods for assigning floor sensor observations to multiple people and for tracking these targets. The author was the corresponding author and he designed the test arrangements and the high-accuracy reference positioning system needed to determine the true locations of the targets.

Publication IV describes in detail the fall detection method using the floor sensor. The author was the corresponding author and he designed the test arrangement and conducted the training session of the algorithm and the test sessions. He was also responsible for analyzing the final results.

Publication V presents the implementation of an add-on capacitive radio frequency identification (RFID) feature. The development of an active capacitive tag placed in a shoe is described. The author was the corresponding author and he designed and implemented the tag and the data-decoding algorithm. He also designed the test arrangements and analyzed the results.

Author's contribution to the technology

The basic concept and specifications for the measurement system were determined by Professor Raimo Sepponen, who was the supervisor of this thesis. On the basis of the specifications, the author had the main responsibility for designing and implementing the measurement hardware. This thesis is a natural continuation from the Master's thesis of the author [1], in which the initial electronic design was done. The hardware is based on that developed in [1], but was completely redesigned to achieve better sensitivity and scalability. The hardware that was developed included a measurement unit and a

multiplexing unit. The author implemented two versions of the measurement unit and the multiplexing unit during the preparation of this thesis. The first versions were put into actual use in the Kustaankartano center for the elderly. The updated version of the measurement unit included support for inductive RFID through the floor and Ethernet and Power over Ethernet (PoE) support. The updated multiplexer had new hi-current output stages for the RFID loops, which are described in [2]. The author has had the main responsibility for initiating and supervising the mass production of this hardware. The capacitive RFID shoe tag in publication V was developed solely by the author.

The author also implemented the embedded software required to operate the hardware in Kustaankartano. This included acquiring and detecting the signals, multiplexing the excitation signal, intelligent scanning patterns, and data communication through a Controller Area Network (CAN). He also made a major contribution to developing the communications protocol between the measurement unit and the computer.

Abbreviations

AC	alternating current
A/D	analog to digital (conversion)
AREF	reference voltage of A/D converter
D/A	digital to analog (conversion)
DAC	digital-to-analog converter
DC	direct current
CMRR	common-mode rejection ratio
CAN	controller area network
CAN+	non-inverted signal wire of CAN bus
CAN-	inverted signal wire of CAN bus
GPS	global positioning system
ECG	electrocardiogram
ELSI	electronic sensor with intelligence
EMI	electromagnetic interference
ESD	electrostatic discharge
FEM	finite element method
IQ detector	in-phase quadrature phase detector
IR	infrared
LSB	least significant bit
NFI	near field imaging
PET	polyethylene terephthalate (plastic)
PIR	passive infrared sensor
PoE	power over ethernet
PVC	polyvinyl chloride (plastic)
QUEST	Quebec user evaluation of satisfaction with assistive technology
RF	radio frequency
RFID	radio frequency identification
SIR	sampling importance resampling
SMD	surface-mounted device
SNR	signal-to-noise ratio
UHF	ultra high frequency (0.3 – 3 GHz)
UWB	ultra-wideband
WLAN	wireless local area network

Symbols

ΔZ_s	impedance change caused by a person
ω	angular frequency (=$2\pi \cdot f$)
C_s	sensor capacitance
C_t	tuning capacitor
f	excitation frequency
I_{R1}-I_{R4}	received currents
I_T	transmitted current
I_1	primary coil current
I_2	secondary coil current
L_1	primary coil inductance
L_2	secondary coil inductance
R_l	load resistance on the secondary coil
R_s	sensor loss resistance
R_1	primary coil loss resistance
R_2	secondary coil loss resistance
R_3-R_4	input resistors of U3
R_f	feedback resistor of U3
R_g	reference resistor of U3
U_ex	excitation voltage
U_out	output voltage of U3
U_2	voltage over the secondary coil load
Z_{LC}	series impedance of the primary coil and the sensor
Z_l	load impedance on the secondary coil
Z_s	sensor impedance
Z_1	primary coil impedance

1 Introduction

The age structure of Finnish society is changing, as the proportion of senior citizens is increasing. This is a relatively new phenomenon, since the proportion of over-65-year-olds was almost constant during the first half of the twentieth century. By the year 2000 it had doubled since the year 1950. This is mostly caused by the increase in life expectancies and the birth of large age groups after the Second World War. [3] Currently, the costs of nursing and care services are growing faster than the gross domestic product in Finland, and the ratio between over-65-year-olds and those of working age will have doubled by the year 2040. The future of municipal economies would be much brighter if work productivity in care services for the elderly was more effective. [4] In this thesis the term care for the elderly is used to cover both the institutional care for the elderly and the care services for senior citizens living independently. The term elderly is understood here as people roughly over the age of 75-80 years and possibly having decreased functional health status. The term senior is used for people roughly over 65-70 years of age with good functional health status.

Remote monitoring has been found useful in care services for senior citizens living independently. In a study by Celler *et al.* it was proposed that functional health status amongst over-65-yearolds living independently could be determined remotely by measuring simple parameters such as mobility, sleep patterns, and the utilization of cooking, washing and toilet facilities in their homes [5]. Also eating habits at home could be monitored by observing visits to the refrigerator [6]. In a study by Alwan *et al.* parameters such as gait, falls, stove usage, and bed exits were measured in the homes of 13 test subjects that were 63-100 years of age. They found that the monitoring actually relieved the caregivers' strain levels and slightly increased the perceived quality of life of the residents [7]. There are numerous examples of sensory data benefiting the elderly living in institutions or their caregivers. People suffering from dementia often wander around, regarding which alarms can be generated [8]. Data indicating presence at meals or in the toilet is useful information for the nursing home staff [9]. The prevention of falls could be made possible by detecting persons getting out of bed or entering the toilet, since a large proportion of falls occur in these situations [10].

One of the greatest problems amongst the elderly is falling. Falls have severe medical consequences [11], and therefore severely affect the quality of life and the costs of care. It was found in a study by Fleming *et al.* that 60% of people over the age of 90 fell at least once a year. The study had 110 participants. In 99% of the cases in which the person could not get up, some form of a call alarm system was present. Still, in 80% of these cases the person did not use the system and 30% of these were left lying on the floor for an hour or more. This result is alarming, especially when keeping in mind that 47% of the call alarm systems in the study were worn personally. [12] This fact forces automatic fall detectors to be developed. To prevent older people from lying helpless on the floor for long periods, the fall detectors should be chosen in such a way that they do not require any actions from the person [13].

In this thesis it is proposed that the care services for the elderly and for the seniors can be made more effective by using the system that was developed. In this work, a novel person tracking method and system based on electric Near Field Imaging (NFI) is presented. This monitoring system aims to increase work efficiency in nursing homes, which are already struggling with the lack of qualified staff. In addition to institutions, the system can also be used in private residences of senior citizens who are on the brink of moving to a nursing home. The system can be used remotely, postponing the need for full-time care. This could lower the costs inflicted on society and could increase the quality of life of senior citizens with some form of impairment.

The sensing system presented in this thesis is called the Electronic Sensor with Intelligence (ELSI), and it is based on NFI technology. A matrix of thin and undetectable electrodes is applied under a floor surface. The spatial distributions of conductive objects near the floor, such as a human body, can be observed. This technology is used here used for multiple purposes: for fall detection, for creating location-related information, for activity monitoring, and for detection of the vital functions of a person lying on the floor. This information can be observed on a computer and it is also used generate automatic alarms. The alarms are sent to the cell phones of the caregivers and they can also be used to control an existing call system. The essential thing in the alarms is that no user input is needed from the person under monitoring and no devices need to be worn.

1.1 Goals of the study

The study has the following goals:

1) to develop a scalable and discreet system for positioning people in an indoor environment and to enable their activity to be monitored;

2) to develop techniques for detecting alarming situations such as falls and unexpectedly entering or leaving the areas being monitored;

3) to develop techniques for detecting the identity of a person and for recording the biosignals of a person who is lying on the floor;

4) to apply the system in institutions for the elderly and private homes of senior citizens to improve the level of care, and

5) to compare the results with related work

2 Related work

Person tracking has risen to a new level of interest since the use of global positioning system (GPS) has become a part of the everyday life of the general public. The fact that GPS does not work indoors forces one to seek solutions from other techniques. Pervasive/ubiquitous computing requires location information to provide adaptive and intelligent services. These include interactive environments, adaptive building automation, passage control, and health care informatics.

These services can generate notifications or alarms about people moving in a certain area at a certain time. They also help to find the person or equipment. Statistical analysis can be used for determining the behavior a person being tracked. Context-related information or adaptive functions can be provided directly to the person being located. Furthermore, location information can be used to assist in navigation.

The techniques that make the services possible can be divided into two categories: active and passive ones. The active techniques use some kind of mobile device, which is carried by the person being tracked. These include radio frequency identification (RFID) tags, cell phones and transponders based on radio frequency (RF) signals, ultrasound, infrared (IR), and so on. The passive ones sense the body of the person itself and do not require a transponder; however, they do not necessarily rule them out if identification is required. These methods include computer vision, passive infrared sensors (PIR), floor sensors, electric field sensors, and so on.

The system developed in this thesis is a combination of a person tracker, identifier, fall detector, and vital function monitor. The related work concerning these fields is discussed below.

2.1 Person tracking and identification

Related work that makes tracking or tracking and identification possible is discussed here together, since the majority of the techniques used are active. The use of a transponder usually means that identification is also provided.

The most common location techniques are summarized in a survey by Hightower and Borriello [14]. The most common way is to use a radio frequency transponder using a wireless local area network (WLAN) such as the Ekahau system [15], ZigBee [16], or a cell phone [17]. The advantage of these techniques is the relatively affordable infrastructure. One only needs a set of base stations for the system to work. The downside is their relatively poor accuracy, which may not be enough to determine if the person is in a certain room, never mind a specific location in the room. The best accuracy is in the scale of 1.6 m [15]-[17]. Furthermore, a mobile device must be carried at all times and the battery must be charged frequently. The use of transponders

for the positioning of the elderly suffering from dementia is difficult, since some irritable patients will not wear such devices and remove them [18]. The upside to most transponder-based systems is that they provide identification automatically.

The use of passive RFID tags worn by the person solves the battery problem [9]; however, then the localization is strongly discrete because the number of reader stations is limited. This cannot be called a true localization system. If a person carries the reader and the tags are placed in the environment, the battery problem occurs again [19], [20]. This is because the device that is worn both reads the tags and transmits the information back to the system with an RF uplink.

Ultrasonic positioning systems are accurate (≈10 cm) [21], but the infrastructure is relatively complex. One room needs dozens of transducers including extensive cabling and the person must carry a battery-operated transponder at all times. Using ultra-wideband (UWB) signals the accuracy is even better (in the millimeter range), but as with ultrasound, multiple beacons are needed in the room [22]. PIR sensors are affordable, but relatively inaccurate, so they are mainly used for activity monitoring [23]. Infrared positioning systems based on active transponders do not provide continuous location information, as the known implementations have sparsely distributed reader stations [24].

Accurate positioning with computer vision is possible with the use of stereo vision [25]. If digital identification is required, a 2D barcode must be worn. The identification range is limited by the camera resolution. With a resolution of 640 x 480 a 2-m range can be reached, provided that the angle between the barcode and the line of sight is no more than 70 degrees [26]. Similar limitations apply with facial recognition [27]. Observing the stride and cadence of a person who is walking can also be used for biometric identification, but the performance is relatively poor (40%) [28]. In spite of their advantages, all methods that use computer vision are vulnerable to shading and require lots of computing power.

The floor sensors found in the literature are almost all based on floor contact sensing, which requires very complex floor structures [29], [30], [31]. The structure may be up to 20 cm thick and the signals are disturbed by wooden flooring materials [32]. The signals can also be missed if the person is of low weight [33]. It is also possible to use a flexible polypropylene film, such as EMFi, which produces a charge under pressure [34]. However, then the floor covering must also be flexible. Other problems with polypropylene films are their price and the ageing of the material. Floor sensors detecting the static charge delivered by the human body are very affordable and feature low power consumption, which is important when covering large surfaces [35]. They use the triboelectric effect between wired polyvinyl chloride (PVC) sheets and the shoes of the person. A person standing still is not detected as he or she must constantly generate more charge by moving. The ability to see the person for a long time is particularly important when observing slow-moving senior citizens.

Biometric identification with floor sensors provides accuracies between 70% and 93% [29], [30], [36]. These results have not been confirmed with test subject groups larger than 20 people. This raises the question of whether they will work with hundreds of people.

Electric field floor sensing was first presented in 1995 by Zimmerman *et al.* [37]. Their system is explained in detail in Section 3.1.1. In 2007 Savio *et al.* suggested a technique in which self-organizing measurement boards are woven into a carpet [38]. This structure is relatively complex and is vulnerable to mechanical wear. In 2009 Valtonen *et al.* presented a system which used a sensor arrangement similar to that of Zimmerman *et al.*, but had multiple floor electrodes [39] rather than only one. They reported that using a receiver electrode on the wall causes a weakening of the signal at the edges of the area. An accuracy of 41 cm with a walking person was reached.

2.2 Fall detection

The usefulness of automatic fall detection in care for the elderly is self-evident. However, the introduction of automatic fall detectors has been difficult because of organizational complexity and a lack of acceptability [13]. The acceptability issues can arise especially when trying to use fall detectors worn by the subject, which can be restraining, or camera-based solutions, which can compromise privacy. The fall detector should have discreet and ubiquitous properties. As a fall itself is difficult to prevent with technological aids, the focus should be on minimizing the time spent on the floor after a fall [13]. After all, two thirds of people over 90 years of age cannot get up on their own after a fall and sometimes lie helpless on the floor for long periods [12].

The most common fall detection techniques are summarized in a survey by Noury *et al.* [40]. Fall detection devices worn by a user, such as accelerometers [41], [42] or gyroscopes [43], have been reported to give excellent performance. Worn devices can even detect the free-fall time before the impact of falling and could employ an inflatable hip pad to prevent a fracture [44]. The downside to worn devices is the fact that some irritable patients with dementia will not wear such devices [18] and the batteries must be changed frequently.

With unobtrusive fall detectors, no batteries need to be changed and no devices need to be worn. These studies usually use a combination of sensors, such as vibration sensors [45], IR sensors [46], or both together [47]. However, these techniques may have problems with low-impact falls or shading. Computer vision is the leading unobtrusive method [48]-[52]. A system based on a single camera has reached a sensitivity and specificity of 93% and 98% [50]; however, no unclear falls such as ending up on one's knees were tested. If unclear falls are considered, the performance typically drops to 77% and 95% [51]. Using eight cameras, a perfect performance can be reached [52].

2.3 Remote detection of biosignals

The detection of biosignals is seldom associated with systems capable of person tracking. Because this feature is present in the system developed in this work, some related techniques found in the literature are briefly mentioned. There are several studies involving the remote monitoring of vital functions. These include high-impedance potential probes [53] and charge amplifiers [54]. These implementations are intended to be used in medical applications where the person is motionless. EMFi electret films can record the cardiac signals of a person sitting on a chair or lying on the floor [55]. However, electret films are limited in size and the material loses sensitivity over time.

3 Methods and implementation

In this section the developed method and its physical implementation is described in detail. Arguments for selecting the method are presented by comparing its properties and potential to related work.

3.1 The NFI method

The NFI detection method has many advantages compared to other methods found in the literature. The first and the most obvious is the fact that no transponder needs to be carried. Thus there are no batteries and no possibly inconvenient devices need to be attached to the body or clothing. Furthermore, the positioning is not restricted to individuals carrying a transponder, as it also reveals the locations of other people.

The only problem with carrying no transponder is that identification cannot take place. However, in some cases, such as in nursing homes, the person can be identified by the spatial context. For example, if a person gets up from a certain bed, their identity can be resolved with good certainty. Sometimes the identity is irrelevant if the people being monitored have separate rooms. In nursing homes the information about a fall or night-time activity is accurate enough if it is localized in a certain room.

If constant identification is desired, the NFI method does not rule it out. There are two independent methods for achieving this. The first does not require any changes to an existing installation; one just needs to add tags to the shoes of the people who need to be identified by the floor [V]. The tags change the electric field so that the system can interpret digital encoding from the same signal as is used for the localization. The second method requires the addition of inductive loops in the NFI sensor films, which send digital information using magnetic fields. This information is picked up by another kind of tag, which is carried by the person who needs to be identified. The information from the loops on the floor tell the tag its location, and the tag sends it forward, together with the person's ID, using a ZigBee radio [2], [56].

One advantage of the system developed in this work is its completely undetectable and discreet nature. The person being monitored is completely unaware of the surveillance, if so desired. If the person is aware of the system, he or she will not have any reminders of its existence. The discreet nature of the system will not raise privacy issues, unlike computer vision. Even though the video feeds are not observed by humans, the cameras may cause an uncomfortable feeling. Furthermore, the processing of the data is easy, because only conductive objects near the floor are detected; there is no need to extract shapes or movement from the background. Changes in the lighting or shadows do not disturb the system, either. Night-time operation does not require special attention or techniques.

The floor structure of the system developed in this work is very simple compared to pressure-sensitive floors. An inexpensive plastic film is glued onto the base of the floor and can be covered with common floor coverings. These include plastic membranes, linoleum tiles, laminate, parquet, and carpets. These coverings do not disturb the signal and are easy on the eye. The cost of the system is approximately $60 per square meter. At the time of writing, the most inexpensive comparable floor sensor system costs approximately $120 per square meter [31].

3.1.1 Measurement problem

Here, electric field sensing is proposed to be used for the tracking of humans or objects with similar sizes and electrical properties. The requirements for the measurement system were the following: it should be sensitive, reliable, and immune to disturbance. Furthermore, it should be scalable and enable a building to be covered completely.

The concept of using the electric near field for detecting the presence of a human body was presented in the mid-'90s by Zimmerman *et al.* [37]. Their focus was on developing a new method for human-computer interaction. Later the same method was used for digital communication with the environment and with other people nearby [57]. Although the basic concept of this thesis is related to the method presented by Zimmerman *et al.*, the electrode arrangement and measurement electronics are dissimilar, which makes the system developed here novel. These improvements are explained later.

According to Zimmerman *et al.*, there are two basic topologies in electric field sensing: the first is to emit a low-frequency electric field into a space and sense it with another electrode. At rest one element detects the displacement current I_{R1}, which is generated by the potential difference between the electrodes. See Figure 1, part a). If a conductive object, such as a human body, enters this space, the object 'steals' a part of the electric flux and channels it away from the sensing element. This proportion of the flux goes to ground through the body and its coupling to ground. It generates the current I_{R3}. The change in the detected displacement current (I_{R1} vs. I_{R2}) reveals the proximity of the person. Zimmerman *et al.* call this method the human shunt method [37].

The second topology is to emit the electric field from a single electrode, which the person can touch or come close to. By doing this the body itself acts as an 'electric field transmitter'. See Figure 1, part b). The displacement current I_{R4} is measured with an operational amplifier configured as a current amplifier. It is connected to the second electrode and the virtual ground at its input attracts the electric field. The displacement current I_{R4} changes depending on how close the person is to the transmitting electrode. Zimmerman *et al.* call this the human transmitter method [37].

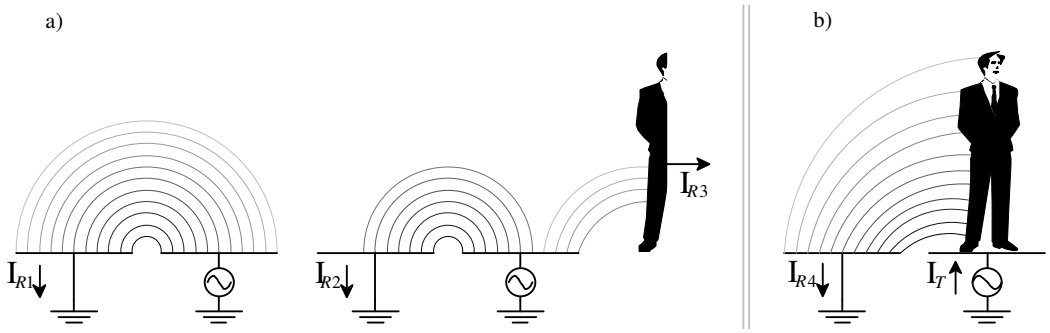

Figure 1. Sensor topologies according to [37]: a) the shunt method; b) the human transmitter method.

The topology used in the system developed here is similar to the human transmitter method. The only exceptions are that the current I_T is measured instead of I_{R4} and the second electrode is grounded to attract the electric field. The reason for measuring I_T instead of I_{R4} is that a single measurement reveals the position of the person as the person's body defines the current I_T. If the receiver current I_{R4} were measured, one would need multiple measurements around the transmitting electrode, which would have to be combined to determine the person's location. This would require more time and more processing.

The reason for not using the shunt topology in part a) is that a separate set of ground electrodes would be required. Grounding is necessary so that the person is able to channel the electric flux away from the sensing elements. The structures of the building could be used for grounding purposes, but this is not acceptable because of the structural variation in the installation sites. In other words, the grounding must be controllable in order to limit the required measurement dynamics.

The other differences between the system developed in this work and the system created by Zimmerman *et al.* [37] are explained next. They used four receiving electrodes on the walls and one transmitting electrode on the floor. See Figure 2, part a). The position of the person is calculated from the relations of the signal strengths received. The signal strength is inversely proportional to the distance cubed, which limits the size of the area being monitored. Furthermore, only one person in the room can be positioned with four receivers. Discriminating between multiple people would require more receivers. The capacitance between the receiver and the transmitter electrode is in the order of picofarads, and the displacement currents are in the order of nanoamperes [37]. With signals this small it is difficult to use multiplexers or long cables, so increasing the amount of receiver channels is relatively complex.

The system that was developed forms electrode geometries similar to [37] by combining small planar elements of a matrix on the floor. See Figure 2, part b). The number of people is then not limited and the sensitivity is not dependent on the distance from the walls. Furthermore, the multiplexing of the signal is easy because the current and the capacitance are in the scale of milliamperes and nanofarads. Thus the system can handle

hundreds of electrodes with one detector, which makes it more scalable than that in [37].

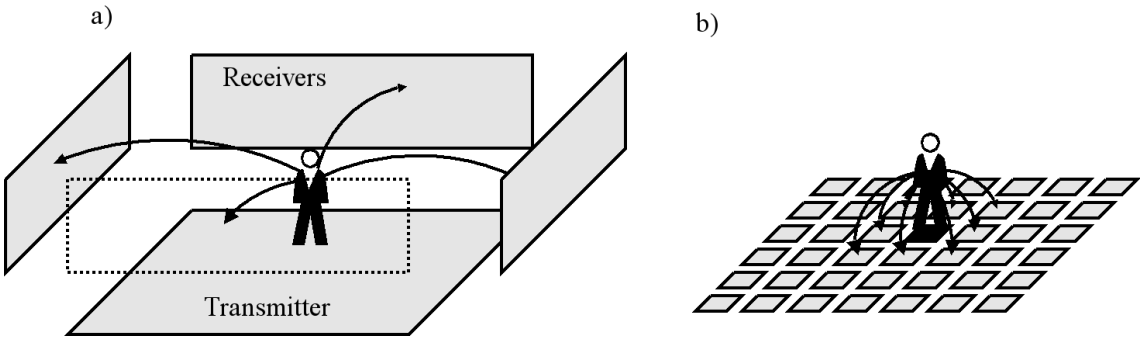

Figure 2. a) The system of Zimmerman *et al.*: the floor is the transmitting electrode and the receiver electrodes are on the wall. The wall electrodes measure the displacement current; b) the ELSI system: the black element is the transmitting electrode and the surrounding elements provide the return path to ground. The current to the transmitting electrode is measured.

The system developed in this work was first presented in January 2008. It was developed without an awareness of the work of Savio *et al.*, who published their work in May 2007 [38]. ELSI has a centralized measurement structure, in contrast to their distributed one, which makes the installation simpler and means higher tolerance to mechanical wear. It also enables a large variety of flooring materials to be used, whereas the system described in [38] is restricted to carpeting. Valtonen *et al.* published their work in 2009, but it had uneven spatial sensitivity [39], unlike the system developed here.

3.1.2 Sensor geometry

The most recent sensor geometry is presented in part a) of Figure 3. It was designed by UPM-Kymmene New Ventures and Elsi Technologies Oy in co-operation with Antti Ropponen and the author. The sensor elements are rectangles with dimensions of 36 cm x 30 cm. Some experiments using inter-digital sensors have been carried out, with no advances in sensitivity. The dimensions were determined by the manufacturing capabilities of the laminating process, which can produce laminates up to 44 cm in width. The sensor consists of aluminum foil with a thickness of 13 µm, which is on top of a polyethylene terephthalate (PET) plastic film. The shapes are made by etching the aluminum. The sensor film is laminated between two additional PET layers to add durability. The total thickness of the laminate is 150 µm.

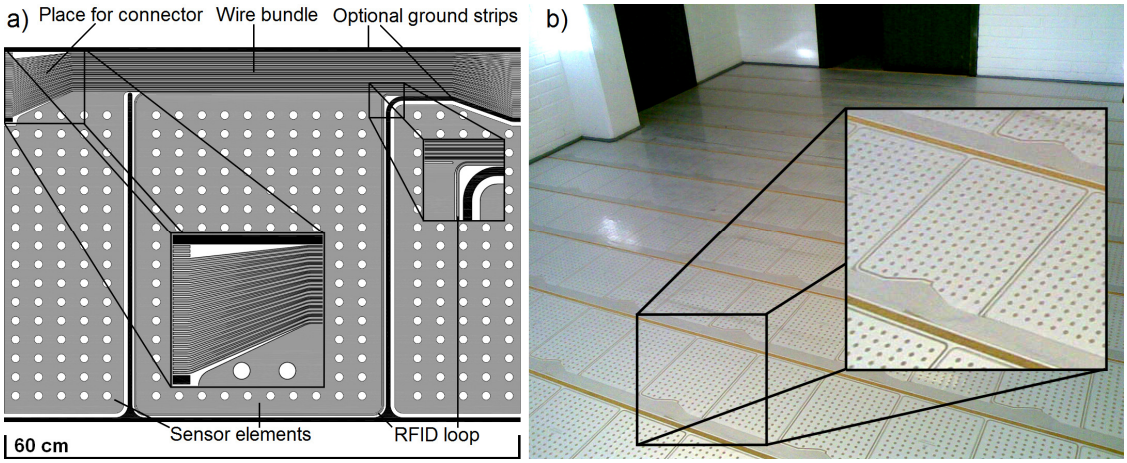

Figure 3. a) The sensor geometry; b) sensors installed on a floor before the floor covering. The magnifications have a scale of 200%.

The sensor geometry is designed in such a way that it can be manufactured in continuous patterns and can be freely cut to size. In part a) of the figure one cycle of the pattern is shown. The laminate can be cut at the vertical edges of the figure. The places for the connectors are at the edges and the connection is made by crimping. The wire bundle is wide at the connector locations and is narrower elsewhere to provide higher coverage for the sensor elements. During one cycle, the wire bundle shifts slightly downwards to make space for the wires of the next cycle. Thus the first element of the cut laminate always has pin number one in the connector. There are RFID transmitter loops around every other sensor element. There are also optional ground strips, which provide a return path for the excitation signal in cases where the implementation of the electronics does not provide it. The implementation presented here does not use the ground strips, because it grounds all the other sensor elements except the one being measured. The holes in the aluminum foil allow the laminate to 'breathe', which allows the adhesive to dry more quickly.

Part b) of Figure 3 shows a room with sensors installed. This site was used in [2]. The sensor laminates come in spools with a width of 44 cm. Therefore several laminates must be positioned side-by-side to achieve full coverage in the room. There is a connector at the end of each film, which is connected to a multiplexer board. The multiplexer boards are chained together and connected to a measurement unit in the corner of the room.

3.1.3 Simulations of the sensor arrangement

Simulations were performed to illustrate the electric flux distributions and impedance levels of the sensor arrangement used in the ELSI system. The COMSOL Multiphysics 3.5a software was used. It is based on the finite element method (FEM). Figure 4 illustrates the geometry used in the simulations. It imitates an actual installation as closely as possible.

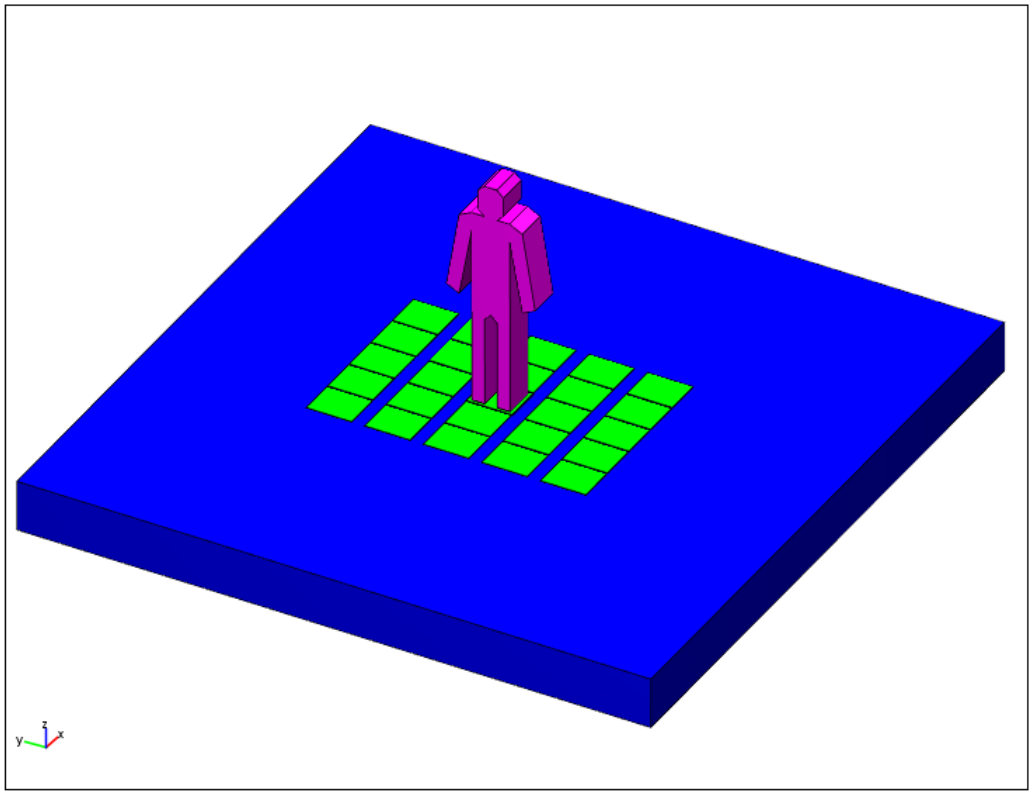

Figure 4. 3D model used in the simulations. The transmitting electrode is at the center and the others are grounded.

The sensors were placed in a 5 x 5 matrix. Larger array sizes were not possible because of the memory limitation of the computer that was used (2 Gb). The sensors were modeled as rectangles with dimensions and pitch as explained in Section 3.1.2.

A block modeling a concrete floor was placed under the sensors. The concrete slab was modeled as a lossy dielectric material. The value for the dielectric constant was chosen to be 250-375i. This is the value for 28-days-old Portland cement-based concrete at 100 kHz [58]. The sensors were modeled as aluminum plates with a conductivity of $37.7 \cdot 10^6$ S/m. A simple geometric model of a person was placed on top of the sensors. The medium inside the person was assumed to be homogenous and to comprise muscle tissue. The conductivity was 0.15 S/m and the dielectric constant was $5 \cdot 10^3$ [59]. The excitation signal had a frequency of 90 kHz. The selection of the operating frequency is explained in Section 3.1.5.

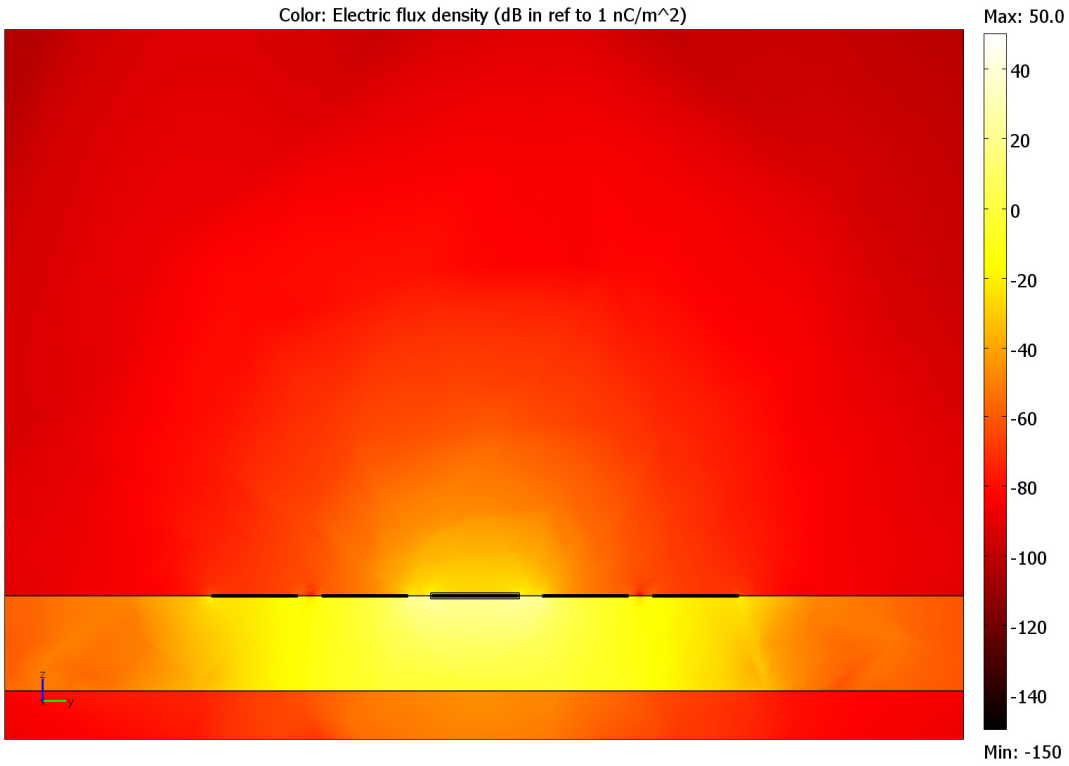

Figure 5. Simulation without a person. The transmitting electrode is in the middle.

Figure 5 shows a situation with no person. The background color shows the electric flux density, which is proportional to the sensitivity of the system. The unit is dB in reference to 1 nC/m^2. A decibel scale was chosen, because otherwise the illustration would not reveal the electric flux density in the air. This is because the concrete slab has a much larger dielectric constant and gathers the vast majority of the electric flux. There is a 53-dB difference in the flux density when the upper and lower surfaces of the transmitting electrode are compared.

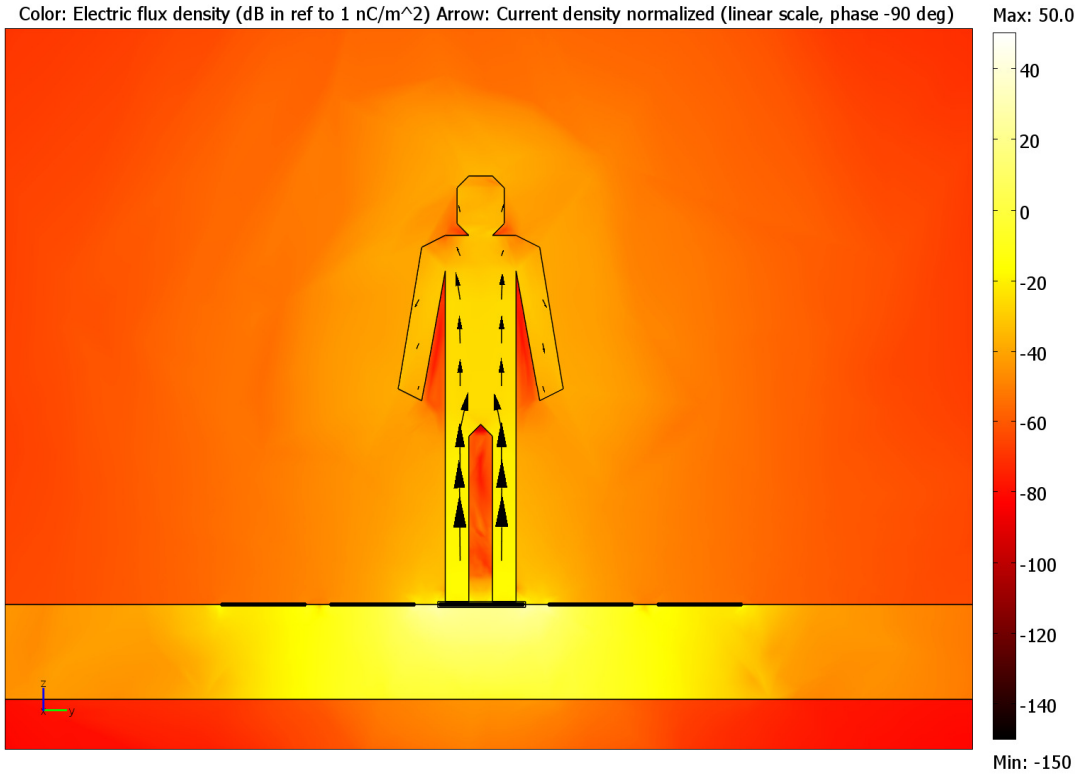

Figure 6. Simulation where a person stands directly on top of the transmitting electrode.

Figure 6 shows the situation where the person is standing on top of the transmitting electrode, with both feet inside its edges. This mode of coupling illustrates well the human transmitter phenomenon described by Zimmerman *et al.* [37]; the person 'lights up' the surrounding air (compare the electric flux density to that in Figure 5). The arrows point the density and direction of the current in the person's body. The length of the arrows is normalized and the scale is linear. They are plotted for a phase angle of -90º as the amplitudes were close to their maximum at this phase. The current flows upwards through both legs and turns downwards when it reaches the arms.

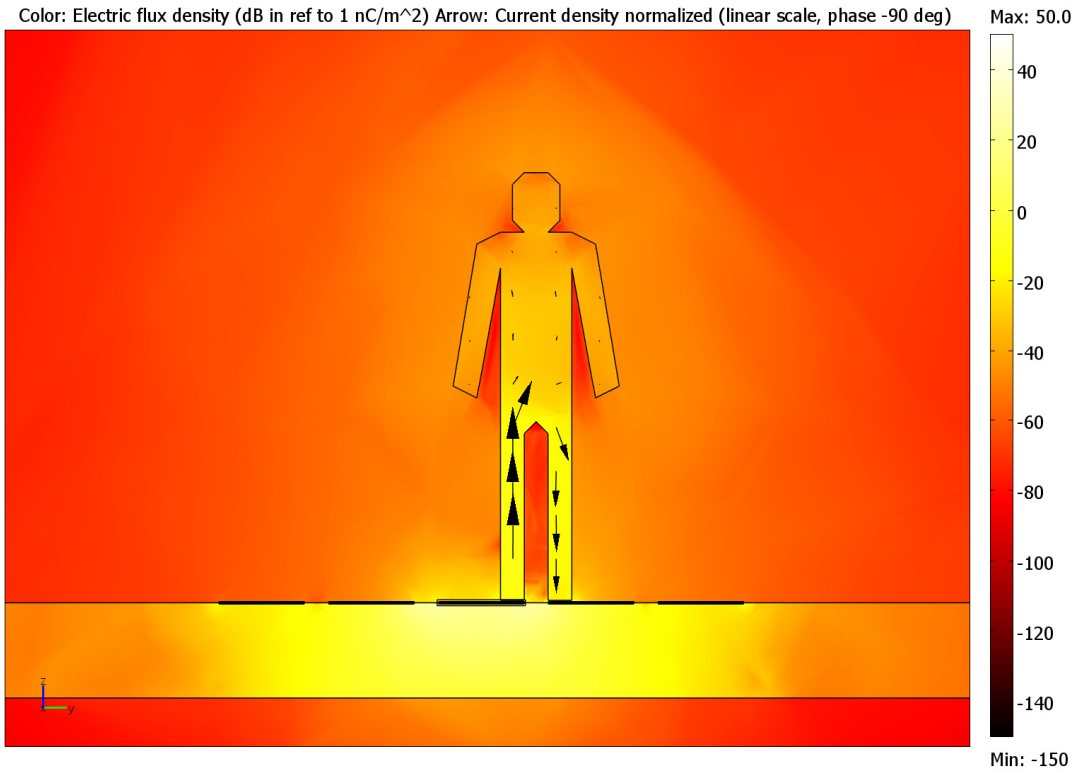

Figure 7. Simulation where the person stands on both the transmitting electrode and one grounded electrode.

Figure 7 shows a case where the person is standing between the transmitting electrode and a grounded one. In this coupling mode, the electric flux density in the air is lower than in Figure 6, as there is a shorter path to ground. The current is shunted directly to ground through the legs and groin of the person.

The rms current density in the leg is 1.2 mA/m^2, which is well below the recommended limit for general public exposure (180 mA/m^2) [60]. Thus the system is safe to use.

Table 1 shows the simulated bulk impedance Z_s of the transmitting electrode and the change ΔZ_s caused by a person. A person forms a parallel impedance between the sensor and the circuit ground, which decreases the overall impedance by ΔZ_s. The table also shows real measurement data for comparison. The three measurements in the table were made sequentially to avoid possible drift of the instrument. The instrument used was an HP 4263A LCR meter, which has a specified basic accuracy of 0.1%. The measurement frequency was 100 kHz and voltage level was 1 V. The test lead was calibrated before the measurement by using the correction functions. A 3 x 3 sensor matrix glued onto a 1.0 x 1.5 x 0.05 m reinforced concrete slab was used. The grade of the concrete was K30 and it had been cured for 30 days on a wooden pallet. 3-mm PVC flooring was glued onto the sensors.

Table 1. Simulated and measured sensor impedances and their changes.

Configuration	Simulated				Measured	
	5 x 5, 20-cm slab		3 x 3, 5-cm slab		3 x 3, 5-cm slab	
	Z_s	ΔZ_s	Z_s	ΔZ_s	Z_s	ΔZ_s
Empty sensor	505.9 Ω ∠-33.8º	-	722.7 Ω ∠-33.9º	-	794.0 Ω ∠-43.6º	-
Person on top of sensor	502.2 Ω ∠-34.0º	4.2 Ω ∠174.5º	720.5 Ω ∠-34.2º	4.5 Ω ∠207.2º	792.3 Ω ∠-43.7º	2.0 Ω ∠157.3º
Person between sensors	504.3 Ω ∠-34.0º	2.5 Ω ∠197.4º	722.3 Ω ∠-34.2º	4.0 Ω ∠229.7º	792.0 Ω ∠-43.7º	2.5 Ω ∠166.6º

The simulated and measured bulk impedances match closely when the results on a 3 x 3 matrix with a 5-cm-thick concrete slab are compared. There is only a 71-ohm difference (794 Ω - 723 Ω), which is presumably caused by slight dissimilarities in the dielectric constants and the concrete reinforcement in the measured slab (simulation had no reinforcement). Since the difference is less than 10%, it is concluded that concrete reinforcement has marginal effect on the bulk impedance. According to the simulation, a 20-cm-thick slab and a 5 x 5 matrix reduce the bulk impedance to 506 ohms. The latter configuration was used in Figures 5-7 and is considered a realistic situation.

The simulated impedance changes caused by a person were 4.2 and 2.5 ohms on a 5 x 5 matrix. When a 3 x 3 matrix and a thinner concrete slab were used, the values were 4.5 and 4.0 ohms. The corresponding measured values were only 2.0 and 2.5 ohms. In the simulations slight displacement of the person altered the impedance change by up to two ohms, which suggests that the resolution was not fully adequate (limited by memory). Thus the simulated impedance changes include some uncertainty. The slight differences may also be caused by the inaccuracy of the model of the human body. In addition the measured impedance changes were at the accuracy limit of the instrument. The absolute values fell in the measurement scale of 10 Ω - 1000 Ω and thus were subject to an uncertainty of one ohm (0.1% basic accuracy).

As described, the impedance change caused by humans is very small compared to the bulk impedance. Therefore the electronic design is very challenging. The electric flux is distributed mainly in the floor, which raises the question of whether the sensor arrangement should be different. The proposed sensor arrangement was chosen in order to make the installation simple and keep the cost of manufacturing low. The author emphasizes that this thesis aims to develop a practically feasible system.

Some experiments were performed to apply a shield layer at the bottom of the sensors. If the shield had exactly the same waveform as the transmitting electrode, the bulk

impedance would increase significantly and the electric field would not enter the floor. The development of the shield structure has been left for future studies by the author.

3.1.4 Electronics overview

There are many ways to implement a capacitance-sensing circuit. The commonly known solutions for measuring electric fields or capacitance can be divided into two categories: the ones which measure voltage or current, and the ones which measure time or frequency. The methods measuring voltage or current include the following: the series impedance method [61], [62] and the current amplifier method [37], which is also known as the auto-balancing bridge method [62]. Synchronous detection is commonly used together with these methods, which is also the case with the system developed in this work.

The methods measuring time or frequency include the following: the basic charge time and RC oscillator methods [63], the switched-capacitor method [64], and integrating oscillators [65], [66]. Though they are accurate, the author has found that the methods measuring time or frequency are very vulnerable to electromagnetic interference (EMI) in a floor sensor application. This is because time measurement methods always require some kind of high-impedance input trigger. This can be, for example, an input of a comparator or a counter. This makes it difficult to use EMI-rejecting input filters. If a filter were used, the edges of the triggering signal would be vague. The time measuring methods are very accurate with small sensors, but often fail when using large sensors with more EMI.

The series impedance method, which was chosen in this study, was found to have high tolerance for EMI. This is an important criterion in choosing the design path because there is a lot of EMI present when sensors as large as this are used. In addition, some designers consider the series impedance method to be the most accurate method for capacitance measurement, but it is also described as the method requiring the highest part count [67].

The circuitry presented in Figure 8 was designed by the author and used in the ELSI system. The circuit starts from the timer output of an Atmel AVR microcontroller (AT90CAN128, Atmel Corp., CA, US), which acts as a waveform generator. It is presented on the far left of the figure. This waveform (square wave) is integrated [68] using U1 to tidy up its spectrum; a triangular wave has lower harmonic levels than a square wave. Using a buffer U2 (SSM2135, Analog devices Inc., MA, US) with good load-driving capabilities, the waveform is fed to one of the sensor elements through the primary coil of transformer T1 and through a multiplexer denoted by ‘MUX’. The circuitry is isolated from the power supply with a DC-DC converter (ASA00AA36-L, Emerson Electric Co., CA, US) to limit the bulk value of the sensor capacitance.

LTspice version 2.21b was used as the circuit simulation software. All the circuit simulations in Sections 3.1.5 and 3.1.6 used the schematic shown in Figure 8.

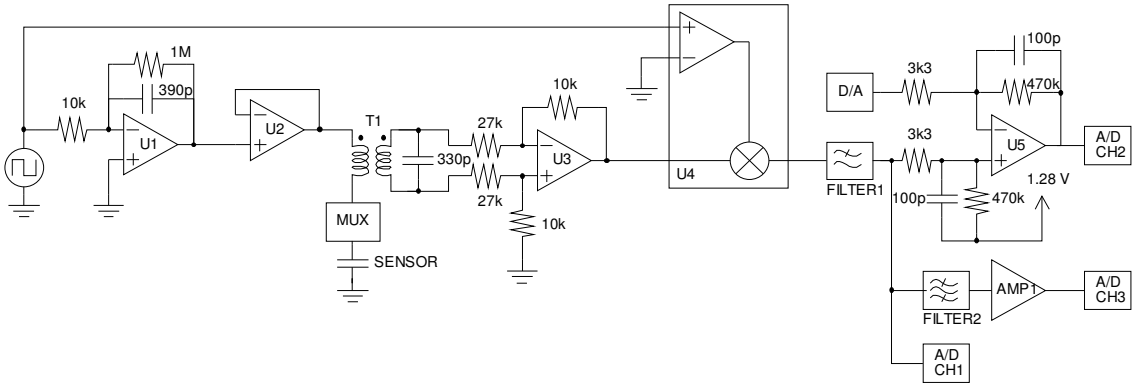

Figure 8. The measurement circuit.

3.1.5 The transformer

The transformer T1 is the core of the measurement. A surface mound device (SMD) coil former was used (Ferroxcube CPVS-ER95-1S-8P, Yaego Corp., Taipei, Taiwan). See Figure 9.

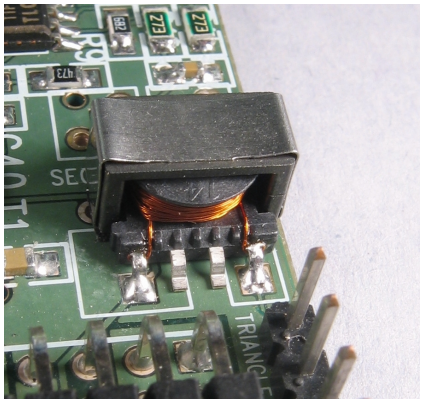

Figure 9. The SMD transformer used in the circuit.

The primary coil of the transformer forms a series impedance, which is used to detect the voltage changes on the sensor. The secondary coil is tuned into parallel resonance with a fixed capacitor. This structure forms a pass-band filter, which rejects EMI. The winding ratio of the transformer is 16:100 (≈1:6) in order to increase the signal amplitude. The effect of the primary coil winding is explained in Section 3.1.6. The primary coil inductance L_1 and resistance R_1 are 239 µH and 0.2 Ω, and the corresponding values for the secondary coil are 8.76 mH and 10.5 Ω (L_2, R_2). The isolation capacitance is 6.5 pF.

U3 is configured as a difference amplifier [68], which converts the differential voltage of the secondary coil back into a single-ended signal. The combination of transformer T1 and U3 offers a high common-mode rejection ratio (CMRR) and isolates the rest of the circuitry from the large sensor array. The interference rejection at the operating frequency was compared by means of circuit simulations to a structure in which the transformer was replaced with a series resistor. The series resistor had the same

impedance as the sensor in order to maximize sensitivity. It was found that the transformer structure had 19% better EMI rejection when the interference was a voltage source and 76% better when it was a current source. The simulations also showed that when the interference frequency is shifted away from the operating point, the advantage of the transformer structure increases.

The operating frequency was selected to suit the sensor geometry and the circuit topology. Higher frequencies decrease the sensor impedance, which is problematic for the driver U2. On the other hand lower frequencies increase the physical size of the transformer as the impedance of the primary coil must be in the same order as the sensor impedance. Otherwise there would be no signal. A good compromise is achieved at a frequency of 90 kHz, which was chosen as the operating point.

The impedance of the primary coil must be in the same order but lower compared to the sensor impedance. At the operating point the primary coil impedance Z_1 is 135 Ω and the sensor impedances Z_s vary from 500 Ω to 3k Ω. Keeping this relation, the series resonance formed by the primary coil and the sensor is at a higher frequency (≈200-400kHz) than the parallel resonance on the secondary coil (90 kHz). If the primary coil were in resonance, its impedance would be equal to the losses of the circuit, as in (1)

$$Z_{\mathrm{LC}} = Z_1 + Z_{\mathrm{s}} = R_1 + j\omega L_1 + R_{\mathrm{s}} + \frac{1}{j\omega C_{\mathrm{s}}} = R_1 + R_s\,, \tag{1}$$

where ωL_1 and $1/\omega C_{\mathrm{s}}$ are equal. This would mean that the series impedance of the primary coil and the sensor element would boil down to a couple of ohms, which would obviously destroy the measurement by overloading the driver U2.

Now we have two resonance peaks shown in part a) of Figure 10. The figure is a simulation with a 1-nF capacitive sensor load. We measure the secondary coil resonance at 90 kHz. The peak at 2 MHz is caused by the primary coil resonance. The primary coil resonance peak would be around 300 kHz if the two resonators had no coupling. As a result of the mutual coupling caused by the transformer, the peak shifts to 2 MHz. The simulations confirmed that the secondary coil resonance at 90 kHz shifts less than 5 kHz when the coupling is varied from 0 to 1. This means that the operating point can be set with the tuning capacitor and the sensor load on the primary coil does not affect it severely.

Part b) of the figure shows a simulation using a more realistic sensor load. This load was modeled as a resistor and a capacitor in series, which had values of 600 Ω and 4.4 nF. This produces the same impedance at 90 kHz as the FEM simulation with a 3 x 3 matrix (Z_s = 723 Ω∠-34º). One can notice that the series resonance at 2 MHz is gone because of the losses of the sensor. The resonance at 90 kHz is still visible, but the quality factor is lower. It is limited by a resistive load, which is explained next.

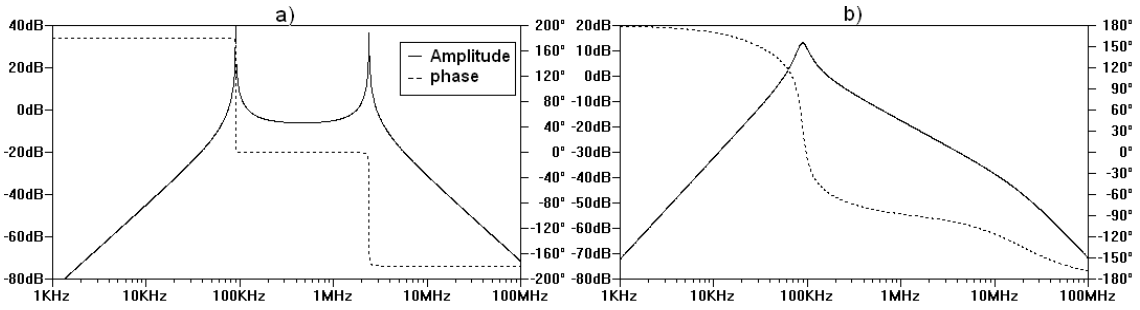

Figure 10. a) Simulated frequency response of the transformer with pure capacitive load; b) frequency response with a typical load.

As the secondary coil is tuned, the optimal operating frequency has to be found by performing a small frequency sweep and maximizing the voltage seen with A/D CH1. The internal analog to digital (A/D) converter of the microcontroller is used. The 16-bit timer of the microcontroller creates the excitation signal, so the adjustment of the frequency is discrete. The adjustment step is approximately 1 kHz around the operating point. The quality factor of the secondary coil resonator is limited in order to make the frequency selection less crucial. The 27-kΩ resistors R_3 and R_4 shown in Figure 11 limit the Q-factor to 10. The figure presents a simplified schematic of the measurement circuit, which is next analyzed in detail.

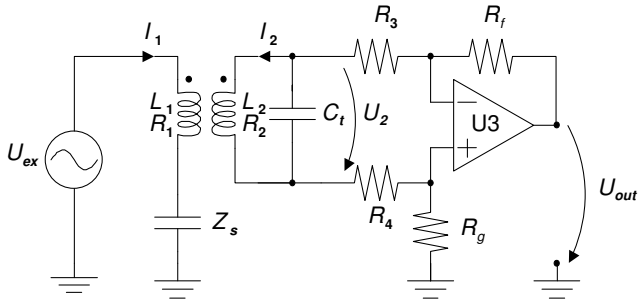

Figure 11. Simplified schematic of the measurement circuit

The output voltage U_{out} of U3 as a function of the sensor impedance Z_s is derived in the following. In a loaded situation the currents of the primary coil I_1 and the secondary coil I_2 have a relationship shown in the equation pair in (2) [69]

$$\begin{aligned} &\text{a)}\ U_{ex} = Z_s I_1 + j\omega L_1 I_1 + j\omega M I_2 \\ &\text{b)}\ 0 = j\omega M I_1 + j\omega L_2 I_2 + Z_l I_2 \end{aligned}, \tag{2}$$

where $M = k\sqrt{L_1 L_2}$ and k is the coupling coefficient of the transformer. U_{ex} is the excitation voltage, L_2 is the secondary coil inductance and Z_l is the load impedance. Z_l is a parallel connection of the tuning capacitor C_t and the load resistance R_l. As the

load is the input of a difference amplifier, R_l can be approximated with the sum of R_3 and R_4 [68] as in (3)

$$Z_l = \frac{1}{j\omega C_t} \parallel R_l = \frac{1}{j\omega C_t + 1/R_l} = \frac{1}{j\omega C_t + 1/(R_3 + R_4)}. \tag{3}$$

The primary coil current I_1 can be solved by using equation a) of (2) as in (4)

$$\begin{aligned} & I_1(Z_s + j\omega L_1) = U_{ex} - j\omega M I_2 \\ & \Rightarrow I_1 = \frac{U_{ex} - j\omega M I_2}{Z_s + j\omega L_1} \end{aligned} . \tag{4}$$

I_1 is then substituted in equation b) of (2) and simplified in (5)

$$\begin{aligned} & 0 = j\omega M \frac{U_{ex} - j\omega M I_2}{Z_s + j\omega L_1} + j\omega L_2 I_2 + Z_l I_2 \\ & \Rightarrow 0 = \frac{j\omega M U_{ex}}{Z_s + j\omega L_1} + \frac{\omega^2 M^2 I_2}{Z_s + j\omega L_1} + j\omega L_2 I_2 + Z_l I_2 \\ & \Rightarrow I_2 \left(\frac{\omega^2 M^2}{Z_s + j\omega L_1} + j\omega L_2 + Z_l \right) = -\frac{j\omega M U_{ex}}{Z_s + j\omega L_1} \\ & \Rightarrow I_2 = \frac{-\frac{j\omega M U_{ex}}{Z_s + j\omega L_1}}{\frac{\omega^2 M^2}{Z_s + j\omega L_1} + j\omega L_2 + Z_l} \\ & \Rightarrow I_2 = \frac{-j\omega M U_{ex}}{\omega^2 (M^2 - L_1 L_2) + j\omega (L_2 Z_s + L_1 Z_l) + Z_s Z_l} \end{aligned} . \tag{5}$$

The voltage U_2 over the secondary coil load can be calculated as in (6) [69]

$$U_2 = -Z_l I_2 = \frac{j\omega M U_{ex} Z_l}{\omega^2 (M^2 - L_1 L_2) + j\omega (L_2 Z_s + L_1 Z_l) + Z_s Z_l}. \tag{6}$$

The output voltage U_{out} of U3 is as in (7) [68]

$$U_{out} = U_2 \frac{R_f}{R_3} = \frac{j\omega M U_{ex} Z_l}{\omega^2 (M^2 - L_1 L_2) + j\omega (L_2 Z_s + L_1 Z_l) + Z_s Z_l} \cdot \frac{R_f}{R_3}, \tag{7}$$

where $R_3 = R_4$ and $R_g = R_f$. The primary coil loss resistance R_1 can be included in Z_s and respectively the secondary coil loss resistance R_2 can be included in Z_l [69]. As the transformer has a ferrite core k can be approximated with 1. Furthermore, (7) is valid

for a sinusoidal excitation voltage, where the actual waveform is triangular. This may result in slight differences, when compared to actual U_{out}.

As explained later in Section 3.1.6, the implementation includes an in-phase quadrature phase detector (IQ detector). Therefore the voltage U_{out} can be observed at 0º phase (I-channel), at -90º phase (Q-channel), or by combining both by taking the norm of both phases. Part a) of Figure 12 presents the simulated frequency responses of these channels at the output of U3. The sensor impedance was taken from the FEM simulations. When the frequency is tuned by maximizing the I-channel, the optimal frequency is at 92.0 kHz. If the Q-channel is used, the frequency is 80.0 kHz. When the norm is being maximized, the optimal frequency is 88.9 kHz, which is the actual resonance frequency of the structure.

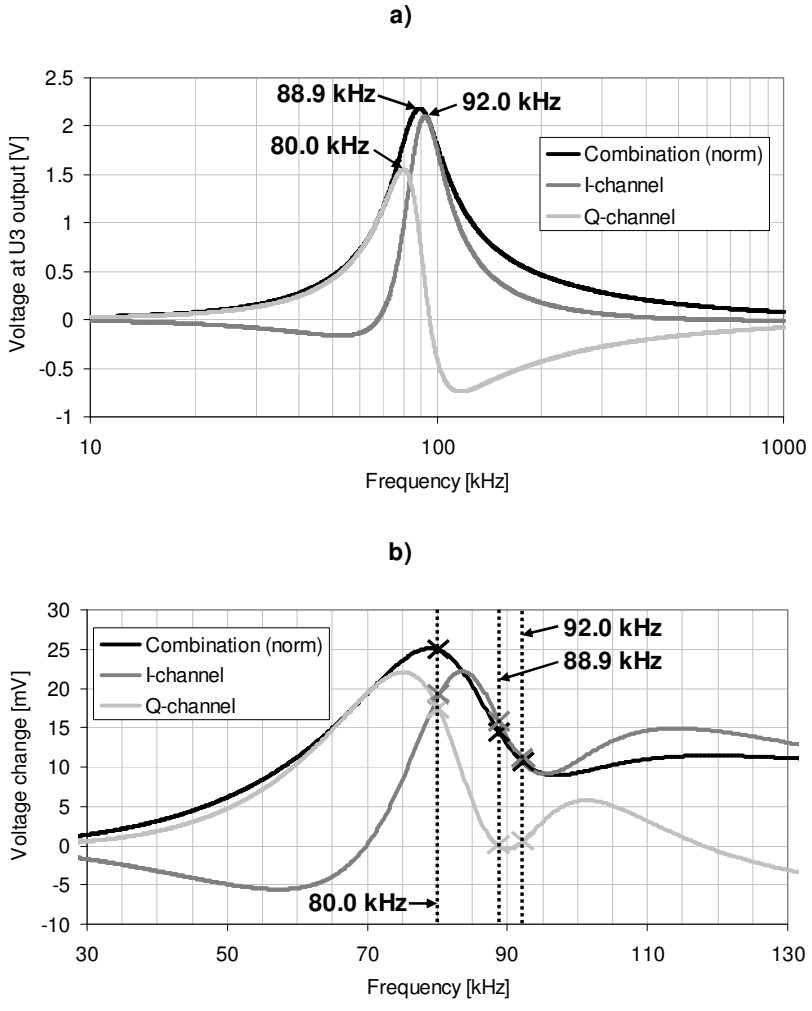

Figure 12. a) Simulated frequency response of the secondary coil. The frequency can be tuned by maximizing the I-channel (92.0 kHz) or the Q-channel (80.0 kHz) or by their combination (88.9 kHz); b) the voltage changes in the above-mentioned channels. The frequencies refer to part a).

Part b) of Figure 12 shows the simulated voltage change when a person stands on top of a sensor. The impedance change was taken from the FEM simulations. It turns out that tuning the frequency by maximizing the voltage of the Q-channel produces the highest sensitivity. This is evident as the voltage changes at 80 kHz are larger than the ones at the frequencies 88.9 kHz and 92.0 kHz.

Table 2 shows the simulated and measured voltage changes at a frequency which is tuned by maximizing the Q-channel (80.0 kHz). The measurements were performed with the system that was developed using a 3 x 3 array on a concrete slab. The simulations used identical geometry. Simulations suggest that the best sensitivity is obtained by taking the norm of the I- and Q-channels. However, measurements show that the I-channel has almost zero sensitivity (0.9 mV) at 80.0 kHz. The sensitivity of the I-channel is also very low at frequencies of 88.9 kHz (4.2 mV) and 92.0 kHz (3.3 mV). Therefore, it is concluded that it is reasonable to implement the detector by using solely the Q-channel. Apparently, the human model in the simulations differs somewhat from the reality.

Table 2. Simulated and measured voltage changes caused by a person on top of a sensor.

Voltage change at the output of U3	Simulated (taken from Figure 12)	Measured
Norm	25.0 mV	16.1 mV
I-channel	18.8 mV	0.90 mV
Q-channel	17.8 mV	16.1 mV

3.1.6 The detector

A phase-sensitive detector was implemented in the circuitry to reject noise and tighten the pass-band [70]. The output of U3 is mixed with a reference waveform by the demodulator U4 (AD630, Analog devices Inc., MA, US); see Figure 8. The actual operation of AD630 is not mixing, but mathematically the outcome is the same. AD630 was chosen because it is capable of operating at a low frequency. The first version of the measurement unit included a full IQ detector using two AD630s. However, in the second version the I-channel was removed because one AD630 costs $17 and the measurements showed that it does not increase the sensitivity; see the underlined result in Table 2. The reference waveform for the AD630 is taken before the integrator U1, which conveniently provides a -90º phase shift, which is needed for the Q-channel.

The phase sensitive detector converts the signal into a direct current (DC) voltage. ‘FILTER1’ removes traces of the excitation signal and residual EMI. It consists of a passive RC stage, which is designed to reduce RF interference, and an active four-pole Butterworth filter, which is implemented using a Sallen-Key structure [68]. It enables easily cascading multiple two-pole filters to achieve higher order filters. It also enables

cascading high-pass and low-pass filters creating band-pass or band-stop filters. The advantages of Sallen-key compared to Multiple Feedback filters is that Sallen-key requires one passive component less and is slightly easier to design. The downside is a weaker stop band rejection. The implementation of FILTER1 is shown in Figure 13.

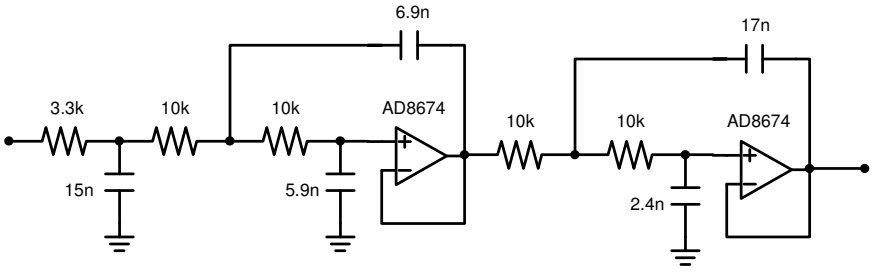

Figure 13. Implementation of FILTER1.

The simulated frequency response of FILTER1 is shown in Figure 14. As the filter also serves as an anti-alias filter, the cut-off frequency must be lower than half of the sampling frequency, which is 4.8 kHz. On the other hand, continuous scanning of the sensors requires fast settling times. Therefore the cut-off frequency is set to the highest possible frequency (2.4 kHz), which results in a 760-µs settling time. This configuration attenuated the excitation signal so that it is not visible with an oscilloscope. However, the attenuation shown by the simulation is probably not reached because of crosstalk.

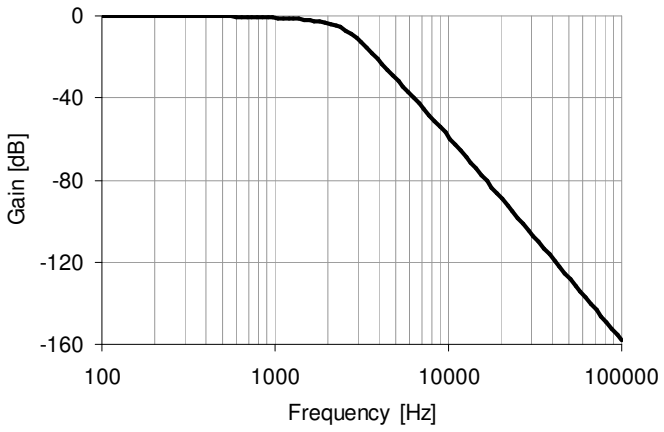

Figure 14. Simulated frequency response of FILTER1.

Now we have a DC voltage which is proportional to the sensor impedance Z_s. This voltage depends on the impedance $|Z_s|$, as shown in part a) of Figure 15. The values in the figure were measured using purely capacitive sensor impedances and observing the Q-channel. Three transformers with different winding ratios were used. The figure also shows predicted voltages for the default transformer (1:6) according to (7). The prediction is slightly higher because the actual U_{ex} is not sinusoidal, but triangular.

Furthermore, at lower impedances the driver U2 can not follow the theory because of severe capacitive loading.

In part b), the curves are differentiated as a function of $|Z_s|$. This tells us the sensitivity of the system. As can be seen in part b), the default winding ratio of 1:6 produces the highest sensitivity at sensor impedances larger than 500 ohms. It has 16 turns on the primary coil and 100 turns on the secondary coil. Below 400 ohms the winding ratio of 1:20 produces the best sensitivity. It has only five turns on the primary coil (and 100 on the secondary) and therefore its primary coil has a lower impedance. As mentioned before, the sensor impedances have been found to vary from 500 Ω to 3 kΩ. Thus the default winding ratio of 1:6 is usually the most suitable. However, if a very low sensor impedance is found, one should resort to a special transformer with a winding ratio of 1:20.

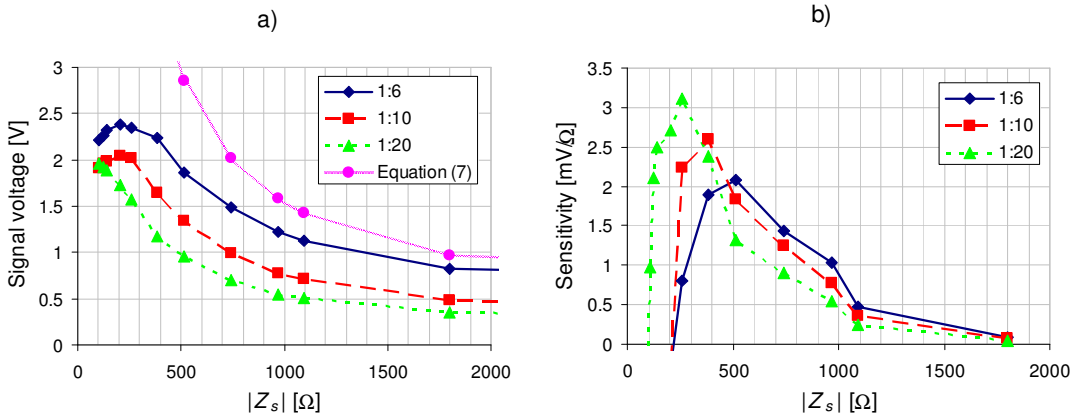

Figure 15. a) Measured detector voltage with different winding ratios b) Sensitivity with different winding ratios. The secondary coil has 100 turns.

After 'FILTER1' the signal is amplified by a gain of 142 with U5, while simultaneously subtracting the bulk voltage with a digital to analog (D/A) converter (AD5331, Analog Devices Inc., MA, US). See Figure 8. Every sensor plate has a different bulk voltage, which is stored in the memory of the microcontroller. A precision operational amplifier was chosen as U5 so that it can handle the large gain and provide low temperature drift (AD8674, Analog Devices Inc., MA, US). The output of U5 is then sampled with A/D CH2 with 8-bit precision. The gain of 142 was chosen so that the resulting rms noise would be close to one least significant bit (LSB) of the A/D conversion.

The circuitry in Figure 8 is also used to detect the vital functions of a person. This is done simply by band-pass filtering and amplifying the DC signal after FILTER1. The filtering is performed with 'FILTER2', which includes one passive high-pass stage, one twin-T notch at 50 Hz [71], and an active two-pole Butterworth low-pass filter, which again is implemented with the Sallen-Key structure. The implementation of FILTER2 is shown in Figure 16.

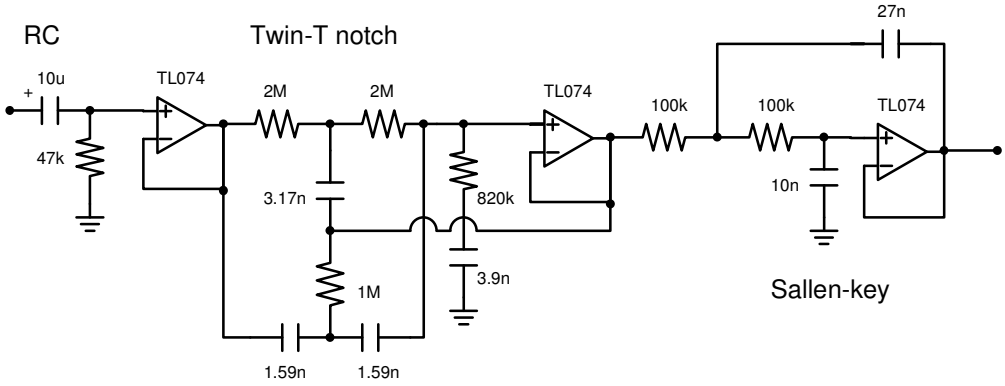

Figure 16. Implementation of FILTER2.

The simulated frequency response of FILTER2 is presented in Figure 17. The filter provides attenuation of 68 dB at 50 Hz and 13 dB at 100 Hz, which are usually the frequencies containing most of the mains interference. The output of FILTER2 is amplified with two stages that have gains of 100 and 34. They are denoted by 'AMP1' and its output sampled with A/D CH3; see Figure 8. The total gain is then 3400 (70dB).

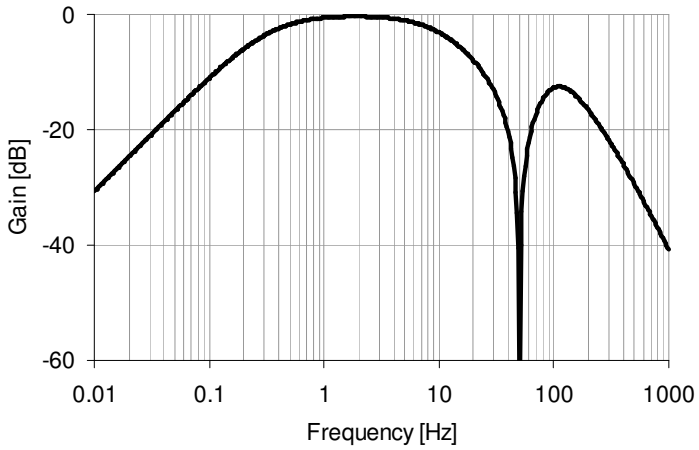

Figure 17. Simulated frequency response of FILTER2.

The multiplexer denoted by 'MUX' in Figure 8 actually consists of several circuit boards that are chained together. Each of these boards is connected to a single-row array of sensor elements. The multiplexers use 20-pin flat cables for communications, power, and for the analog measurement signal. The control data are transferred as parallel bits to avoid using any 'intelligent' components in the multiplexers. The other reason for using parallel data is that serial communications over long cables require differential signaling and complex protocols.

3.1.7 Physical implementation of the measurement unit

The first implementation of the measurement electronics is presented in publication I. During the work on this thesis the author designed a new version, shown in Figure 18. The new version corrected one known bug (an undersized DC-DC converter) and brought in several new features. The old version communicated through a Controller Area Network (CAN), which was changed to Ethernet. This was done in order to minimize the need for custom cabling and special equipment. The new version also had to be powered through the data cable, like the old one, so a Power-over-Ethernet (PoE) interface was implemented. This was done by using an LM5037 (National Semiconductor Corp., CA, US) PoE controller. The Ethernet interface was implemented by using an ENC28J60 (Microchip Technology Inc., AZ, US).

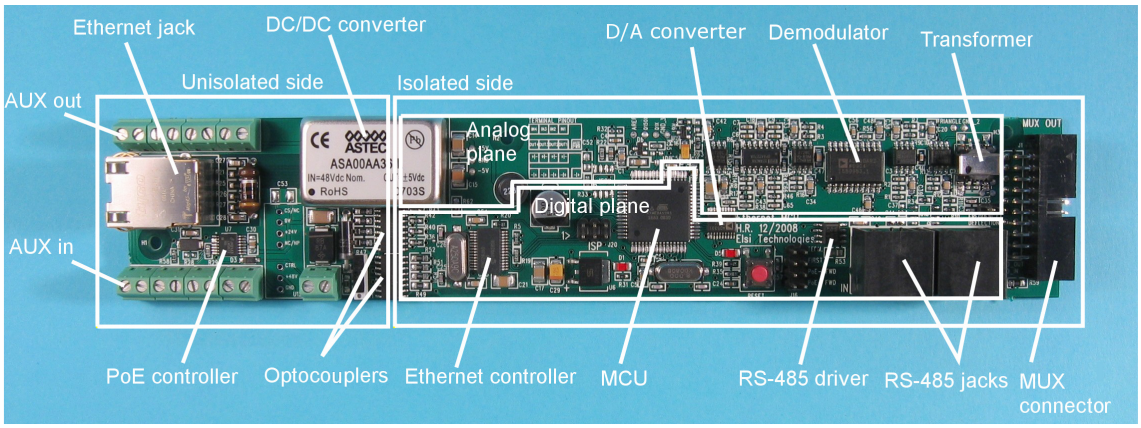

Figure 18. Implementation of the second version of the measurement unit. The dimensions are 218 mm x 41 mm. The first version is shown in publication I.

The new version also had to have a platform for a call system, which includes buttons and lights. This was achieved by placing four auxiliary inputs and outputs with optocouplers on the board. In addition to the call system, the new measurement board had to be able to form miniature networks inside an apartment with several rooms. With Ethernet this is possible, but it requires routers, which take up space and need separate power sources. To form chains of several measurement units, a differential RS-485 bus was used. The pinout for the cables was chosen to be such that the power provided by PoE can be forwarded to all the units on the RS-485 bus. The measurement circuitry was kept the same as the old version, because it had proved to work well.

3.1.8 Detection algorithms

The electronic circuits presented in the previous chapter do not work without embedded software. The embedded software used in the actual installations in Kustaankartano center for the elderly was written by the author. It consists of 2200 lines of C-code compiled into embedded machine language with the CodeVisionAVR compiler. An 8-bit AVR microcontroller unit was used as the embedded platform. This chapter reveals the signal detection section of the code. Communications and other sections are

left out of this thesis. Figure 19 shows the flow chart beginning from the system start-up.

The basis of human detection by NFI lies on the fact that the signal rises, when a person is present and the signal stays up, until the person leaves. A typical signal caused by a person causes a step about 70 times higher than the rms noise since the signal-to-noise ratio (SNR) is 37 dB [I]. This sounds like a simple detection task. However, there are several things that need to be taken into account before one can set a threshold and detect the signal.

First of all, every sensor element has a different bulk capacitance, which affects the optimal operating frequency. This is the case even though the secondary coil is tuned with a fixed capacitor. The frequency must be found by performing a sweep on each sensor during the system start-up. When each of these operating frequencies is found, it is stored in the memory of the microcontroller and is recalled whenever the corresponding sensor element is measured again.

As mentioned above, every sensor element has its characteristic bulk capacitance. Not only does this affect the operating frequency, but it also produces an individual bulk voltage for every sensor element. It must be subtracted from the signal before amplification. Otherwise there would be severe clipping. The subtraction is performed by using a D/A converter (DAC) and a difference amplifier. The DAC voltage is incremented sequentially until the output of the difference amplifier reads exactly half of the A/D reference voltage (AREF). The value of the DAC is then stored in the memory of the microcontroller and fetched every time the same element is measured again.

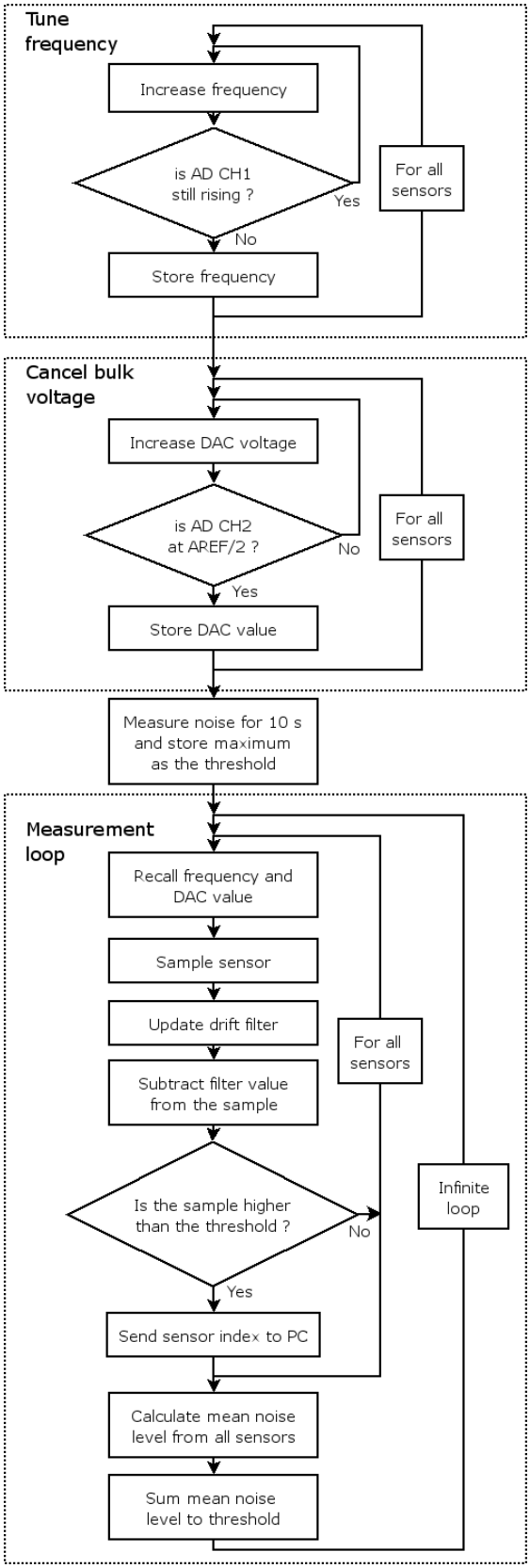

Figure 19. Flow chart of embedded software

Now we have an amplified DC voltage, which corresponds to the impedance of each sensor element. However, there is significant drift present, which is mainly caused by the ferrite transformer core. This has been confirmed by comparing signals with a ferrite core and with an air core. With the air-cored transformer the number of windings was increased so as to achieve identical electrical properties. The net drift of the amplifiers and other active components is negligible because of careful component selection. The drift must be canceled before the detection. This is done by filtering each sensor element with a very slow digital high-pass filter. This cancels the effect of drift, but also cancels observations of people who do not move for a long time. This sacrifice has to be made if one does not wish to see constant phantom observations. The normal time it takes for a person to 'fade away' is a couple of minutes. This rate is suitable compared to the drift rate in extreme situations. An extreme situation could be a window opening in the winter. Furthermore, the drift filter must be asymmetrical. This is required in a case when a person stands still for five minutes and fades away. After this he or she moves to another location and is visible again, but a friend steps on the spot he just left. Now this friend is not seen, because the spot is still blind. If the filter is asymmetric, the faded spot will gain its sensitivity quickly after a static object has moved away. A good value for the asymmetry has been found to be ten. So the filter is ten times faster when regaining sensitivity.

After the operating frequency, bulk voltage, and the drift have been taken into account, one needs to set a detection threshold. A suitable value for the threshold must be measured. The only way to do this properly is to scan the entire floor for a certain period of time, and take the maximum noise peak found. Ten seconds at the startup of the system is used for this. A user-defined threshold is also summed together with the measured threshold. This has been found useful in situations where the automatic noise measurement does not produce a high enough threshold.

At this point the detection ability of the system is quite good. However, there are some cases where additional precautions are still needed. For example, when fluorescent lights are turned on, the noise level of the electronics can rise temporarily. This is caused by voltage surges in the supply line. To avoid false observations, the software must be able to raise the detection threshold fast. The drift filters would do the job if they were allowed to move quickly enough, but they are not. After all, we must detect people. The only way to raise the threshold quickly is to use a spatial average of a single scan. When we take the average signal change of the whole room and sum it together with the current threshold, a couple of people will not be able to raise the threshold. They simply do not activate enough sensors. But when the noise level of the measurement unit rises suddenly, all the sensors are affected. This causes the detection threshold to rise and prevent false observations. Figure 20 summarizes the detection of the NFI signal.

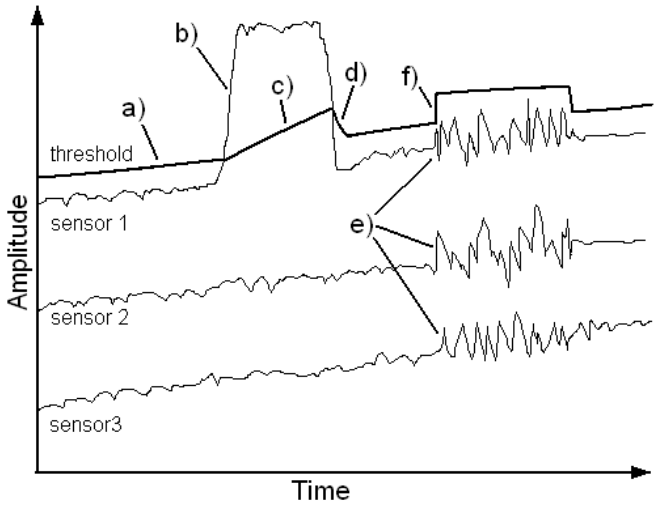

Figure 20. Principles of signal detection. a) The threshold follows the contour of the raw signal as it is tied to the drift filter; b) as a person steps on sensor 1, the threshold is exceeded and an observation is generated; c) the observation starts to fade away as the threshold rises slowly; d) the threshold drops rapidly after the person steps away because of the asymmetry of the drift filter; e) the noise level rises in multiple sensors when conductive EMI is present in the voltage supply; f) by observing the average deviation of all sensors, the threshold can be raised quickly.

Using the detection techniques mentioned above, a satisfactory reliability level was achieved. In the test room it was recorded that no false observations occurred during a weekend, when no people were present. Before and after the 58-hour test period, the system had full sensitivity. Since the update rate of the floor is 4.5 Hz, there were 939,600 updates during the test. If there had been one false observation, the false detection probability would have been $1/939600 = 1.1 \cdot 10^{-6}$. As there are no tests of longer duration available, it is estimated that the probability of false detection in the test room is less than one in a million. The mean detection probability among five test subjects was found to be 0.916 [III]. Considering that in the same room the SNR was found to be 37 dB [I], the probability should be nearly 1 [72]. The reason for not achieving this is that 19% of the sensor area is covered by sensor wiring and gaps between it, which are insensitive to human proximity.

3.2 Pilot installation in Kustaankartano

During the Master's thesis of the author [1], the system was found to be functional in the lab. However, this did not guarantee its functionality in the real world or the feasibility of the intended applications. Therefore the technology was piloted in an actual home for the elderly. We had the opportunity to do this in the Kustaankartano center for the elderly in Helsinki.

3.2.1 Test room at Aalto University

First, a copy of a room at Kustaankartano was built in the Applied Electronics Laboratory. The same sensor film and floor covering were used as what was to be used in the major installation in building 'G'. The room was completely covered with the sensors and had a grid of 9 x 16 elements and a 3 x 3 element grid at the door. The test room proved to be an irreplaceable aid during the whole of this thesis. Almost every test arrangement was set up in this room before being put into practice. The majority of the measurements in publications I – V were made in this test room. The installation of the NFI sensor films in the test room can be seen in Figure 21.

Figure 21. Test room installation on April 28, 2006.

3.2.2 Two-room pilot in building 'A'

Before the major installations in building 'G' began in the fall of 2007, a smaller two-room pilot was set up in the neighboring building 'A', which functions as a hospice for the demented. Both of the rooms had two residents. The small pilot was set up to tune up the usability of the system and get rid of the teething problems. The system was configured to detect falls and residents exiting from their beds, and to identify people with shoe tags. The piloting section in publication V was performed in the two rooms of building 'A'. The architecture of the ELSI system in building 'A' can be seen in Figure 22. This structure was found to be feasible and working and so it was used in building 'G'. The buttons were not installed in building 'G' as there was an existing call button system, which was used for acknowledging also the ELSI alarms.

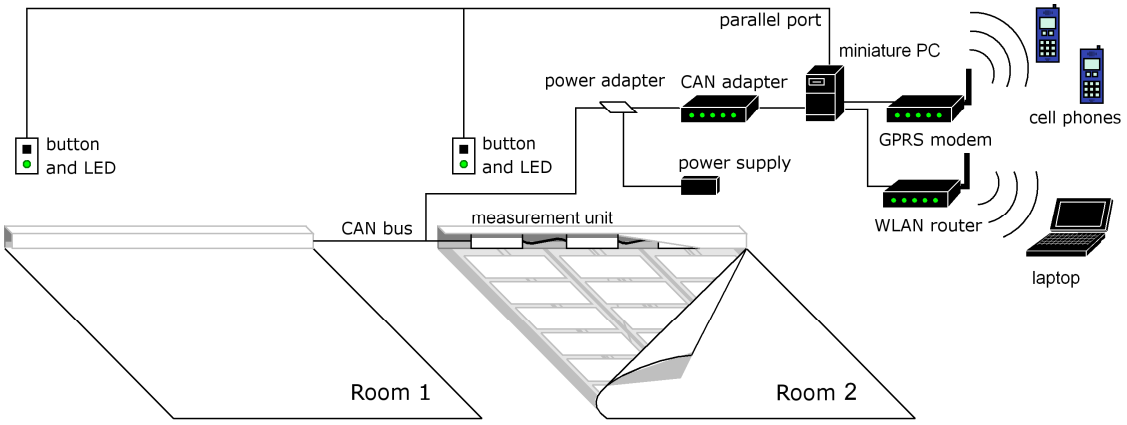

Figure 22. System architecture in building 'A'.

The teething problems in building 'A' consisted of failing power sources, phantom observations, and usability issues in the software. The development of the latter is left out of this thesis. The issues concerning the power sources were resolved simply by doubling the power capacity of the power unit after every failure. The phantom observations were mainly induced by air bubbles beneath the floor covering, and by connector failures, which were caused by oxidation in the aluminum sensor laminates. The connector failures appeared as erratic jitter in the signal. These problems were tackled by piercing the bubbles on the flooring material and excluding the sensors with oxidation in the connectors. The remaining disturbance issues were resolved with various software filters. To avoid the oxidation problem in future installations, the replacement of the aluminum conductors by copper ones is being considered, and the connectors will be cast in epoxy.

3.2.3 Sixty-six-room installation in building 'G'

As the feedback from building 'A' was positive, the installation procedure in building 'G' at Kustaankartano began as a part of full renovation. The building has 64 residents and roughly half of them are in long-term care and are suffering from dementia. The other residents are in short-term care and have physical impairments or are recovering from some form of crisis.

The scale of the installation was large, as there were 66 rooms/areas to be covered with the ELSI system. Figure 23 shows one floor of the building. The circular symbols show each room/area covered with the sensors (22 per floor). The average room in building 'G' has one measurement unit and nine multiplexer units. This means that there are, on average, nine rows of sensor elements in each room. There is 320 m^2 of sensored area and approximately 2300 sensor elements per floor, and there are three identical floors in the building. Thus the building has a 7-kpixel resolution for person localization.

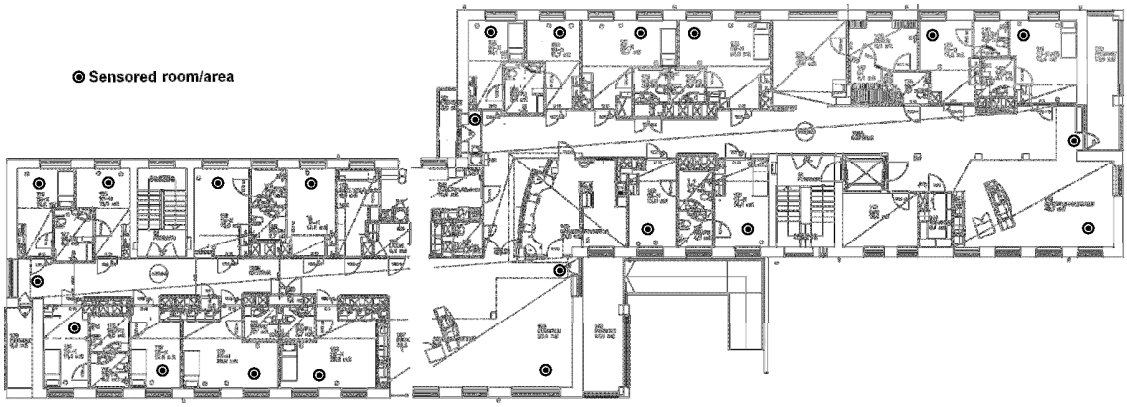

Figure 23. One floor in building 'G' in Kustaankartano. The circular symbol represents a sensored area.

Two automation technicians were hired to install the sensor electronics. They were given two days of training by the author, and completed the task independently. The sensor films were installed by carpeting professionals after a one-day training session. The data and power cables were installed by electricians, as were the power supplies. The data and power networks were inspected and debugged by the author. To do this a custom cable tester measuring three parameters was built by the author. These parameters were the continuity of both differential channels (CAN+ and CAN-) and the presence of a termination resistor. The last parameter also revealed short circuits between the differential channels when termination resistors had not yet been installed.

There were a total of nine error types and eighteen error occurrences in the whole installation process. The most common was an incorrectly assembled female RJ45 connector in the CAN wiring. These errors constituted 6 of the 18 errors. The assembly of an RJ45 connector should be a routine operation for electricians, but apparently that is not always the case. The second most common error was an incorrectly installed flat cable between the circuit boards (3/18). The author learned that if such a cable *can* be connected incorrectly, it *will* be connected incorrectly. In the future circuit designs this will be taken in account.

To date the ELSI system has been officially taken into use on all three floors and the system is functional. The staff uses it during their everyday routines.

4 Summary of publications

In this section the contents of publications I to V are summarized. In publication I the technical solution and the operating principle of the system are described. Some basic properties are measured and presented briefly. In publication III the system is characterized more precisely. The positioning accuracy and the ability to discriminate multiple targets are determined by measurements using a test group of five people. In publication II the biosignal recording performance of the system is determined using a test group of five people. Publication IV presents the fall detection feature. The fall detection ability is determined by measurements using a test group of ten people. Publication V presents a way to provide identification information to accompany the location information. The development of capacitive RFID tags embedded in shoes is presented.

4.1 Human tracking using near field imaging [I]

In the publication the system that was developed is described in detail and some basic performance indexes are measured. These include SNR, linearity, and the signal's dependency on the impedance change. Also some actual location data is presented and it is proposed to be used for creating care services for the elderly.

A human body phantom was created to provide a reproducible stimulus for the system, which can be used for comparing different installation sites. This stimulus was used to measure the SNR of the system. The average response was 22.0 Ω and the average noise level was 0.31 Ω. This corresponds to an SNR value of 37 dB, which matched the result with real test subjects. This was concluded to be more than adequate for person-tracking purposes. The linearity of the measurement system was also verified by connecting a series of known impedance values parallel to one sensor element and recording the results. A linearity error equal to one LSB of the A/D conversion was found. The correspondence between the signal and the impedance change was -2.3 LSB/Ω at a sensor impedance of 1.9 kΩ.

4.2 Biosignals with a floor sensor [II]

This publication presents the vital function monitoring capability of the system that was developed. In some cases it would be beneficial to monitor the vital functions of a person lying on the floor. These include vital sign detection of a senior citizen who has fallen at home. Another application is seclusion monitoring of the intoxicated.

The vital function measurement can be performed at any point inside the area being monitored. The vital functions include respiration and, in some cases, even cardiac activity.

The biosignals recorded with the NFI floor sensor were analyzed, using a test group of five people. Every test subject was measured in four different postures and with two measurement points in each posture. The postures were prone, supine, left lateral, and right lateral. The measurement points were at sternal height and at abdominal height. A time domain integration method was used to extract periodic waveforms from the raw signals, while an ECG signal is used as a trigger for windowing. This was done to determine if the waveforms were definitely caused by the activity of the heart. An example of a clear cardiac signal recorded with the ELSI system is presented in Figure 24. The periodic peaks in the signal are in phase with the ECG signal, which proves that they are caused by the heart.

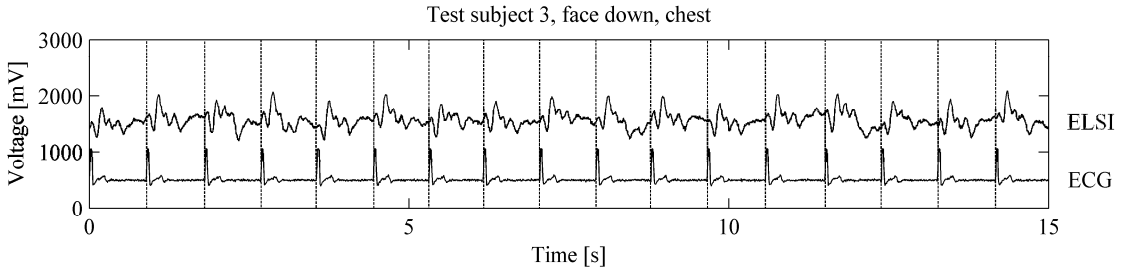

Figure 24. Cardiac signal of one test subject. He was lying prone and the signal was recorded at chest height.

The most favorable posture for cardiac monitoring is when the test subjects are lying prone on the sensor floor. The conclusion was also drawn that people produce similar waveforms in the same postures. The respiration activity is also clearly visible in the signals when the recording point is at abdominal height.

4.3 Positioning accuracy and multi-target separation with a human tracking system using near field imaging [III]

The publication presents properties of the ELSI system, which concern the human tracking aspect. These include positioning accuracy and multi-target discrimination performance. The observation rate (hit rate) is another important measure of the system's reliability. It is the proportion of times when a person is detected while present in the area being monitored. A study determining the same properties has been carried out with a pressure-sensitive floor sensor [33]. At the time of writing of publication III these properties had not yet been measured with an electric field-sensing floor sensor. This fact created a perfect setting for a comparative study between a pressure-sensitive and electric field-sensing floor sensor.

Other studies in the literature have used simplistic experimental settings. This has been done, for example, by asking a person to walk along a line on the floor and maintain a uniform speed. This estimate was not satisfactory for the author. This is why a reel-based triangulation system was developed and used as the reference positioning system. The reference system consists of three actual reels in the top corners of the test room. The reels hold multi-fiber fishing line with high strength and low weight. These lines join at a node which is tied to a hat worn by the test subject. The reels are spring-loaded to keep the lines tight. The positioning measurement is performed by reading precision potentiometers placed in the reels. It was found that the reference positioning system produces a mean error of 2.5 cm in the 19-m^2 test room.

The positioning accuracy was measured by comparing the reference location to several location estimates calculated from the floor sensor data. The estimates were the following: raw observation, observation centroid, and centroid filtered with a Kalman filter [73]. A location estimate based on a particle filter using sampling importance resampling (SIR) was also tried out [74], but it did not provide an advantage compared to a Kalman filter. The multi-target discrimination performance was studied with two people and a Rao-Blackwellized Monte Carlo data association algorithm [75].

The positioning accuracy test was performed with a test group of five people, who each performed three separate test walks at different walking speeds. The mean positioning error was found to be 21 centimeters. The multi-target discrimination test was performed by recording two people walking in the same space on different occasions. These data were then combined as if the people were in the room at the same time. This made it possible to calculate a continuous discrimination performance curve as a function of the distance between the two people. The discrimination performance was found to be 90% when the distance between the two people was 0.78 meters. With a distance of 1.1 meters the discrimination performance was 99%. The average hit rate was found to be 91.6%. It was not limited by the sensitivity, but the gaps between the sensor elements.

The accuracy and discrimination results were exactly the same as those achieved with a pressure-sensitive floor sensor found in the literature [33]. This is a very good result, considering that the pressure-sensitive floor sensor had a resolution four times better than that of our system.

4.4 Detection of falls among the elderly by a floor sensor using the electric near field [IV]

The publication determines the fall detection performance of the system that was developed. Automatic fall detection shortens the time spent helpless on the floor if the person is not able to get up after a fall. It also minimizes the response time of the caregivers, meaning that help is provided swiftly. Fall detectors that are worn by the person perform very well, but require constant changing/charging of the battery, and

some irritable patients remove these devices. This creates a need for unobtrusive fall detection.

Because the sensors are placed on the floor, the system provides particularly favorable data to detect falls. The data only reveals body parts in close proximity to the floor. This lightens the load on computers, since the Z-axis information (elevation) does not have to be extracted from e.g. video imagery. Furthermore, furniture or other people do not shade the signal. Typical data obtained from the system that was developed are shown in Figure 25. A person is lying on the floor with their arms spread wide.

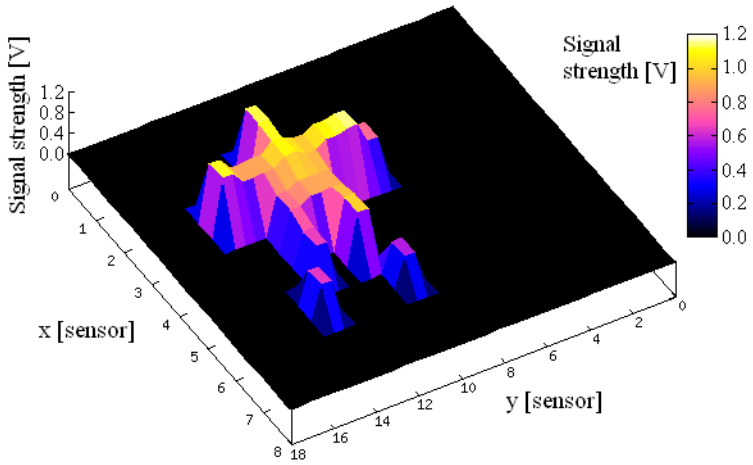

Figure 25. A typical signal pattern produced by a person who has fallen. The data were recorded with the system that was developed.

A test arrangement suggested by Noury *et al.* was used [40], since it is one of the best-known test arrangements for fall detectors. In this way the results are comparable with a large portion of related work. Furthermore, the test arrangement included 650 repetitions, which should ensure statistical significance. A test group of ten people with even gender distribution was used.

Two classes of events were compared; fallen and non-fallen. A classifier based on Bayesian filtering [76] and a Markov chain state model was developed. The sensitivity and specificity of the system were found to be 91% and 91%, respectively. This result is comparable to single-camera computer vision [50].

4.5 Human identification and localization using active capacitive RFID tags and an electric field floor sensor [V]

The publication presents the implementation of an add-on identification feature, which is based on active capacitive RFID tags. In most cases the identity of the person being tracked is evident from their location. For example, in nursing homes the residents have

their own rooms. However, the distinguishing of staff members from the residents requires identification information. One application based on the identification is to turn off new alarms when a staff member arrives and to acknowledge existing alarms.

The tags modulate the impedance between sensor elements on the floor by switching the connection between antenna plates in a shoe. The modulation creates digital encoding, which includes the ID number of the user. The tags were implemented using a low-power microcontroller, which is motion-activated to save batteries. The electronics were cast in epoxy and embedded in shoes.

First, the operation of the tag was characterized by measuring the SNR and its dependency from the distance from the surface of the flooring material. The flooring material on top of the sensor elements was 3 mm thick. A maximum SNR of 17 dB was found when the tag was touching the floor. The maximum read range was found to be 5 mm.

The success rate of the tag-read operation was measured in a fixed location with optimal placement and also in random locations. Both tests included 100 repetitions. In the fixed location, the success rate was 100% and the latency was 0.4 seconds. In a random location, the success rate was 93%. The success rate was also measured in a field test in a nursing home, which lasted for two weeks. Two nurses wore the tagged shoes during their normal work routines. This test yielded a success rate of 93% with a mean latency of 36 seconds. The high latency was because the nurses move around a lot until they stand still for the first time.

The results were considered promising, but it was concluded that fixed footprints on the floor should be used, on which the person must step. This should ensure a high success rate and a low latency.

5 Discussion

The results in publications I – V show that the use of electric fields for detecting presence, movement, falls, biosignals, and the identity of people is feasible. In the following sections these features are compared in detail to related work. The user experiences of the nursing home staff and one senior citizen living independently are also discussed. Furthermore, ongoing and future study directions are discussed briefly.

5.1 Sensitivity and reliability

The sensitivity is an important parameter for the technical characterization of the system developed in this work. SNR was chosen to measure its sensitivity. An SNR of 37 dB was measured in real-life conditions. An electric field sensor developed by Valtonen *et al.* reached an SNR of 27 dB and it had a strong dependency on the distance from the receiver electrode [39]. The system developed here produces virtually even SNR values across the whole room, because no separate receiver electrode is needed.

The sensitivity was concluded to be more than adequate for detecting the proximity of a person. Furthermore, the person is detected regardless of the type of shoes they are wearing; sneakers, loafers, sandals, and even wooden clogs have been found to work.

Detecting the presence and absence of a person is possible with the system developed here. This enables for example detection of getting out of bed and exiting from the room, when the point of appearance or disappearance is observed. At any given moment the certainty of detecting the presence of a person is 92% [III], which is limited by the sensor coverage and the gaps between the sensors. However, when people move around, the certainty increases to close to 100% as they eventually step on a sensor element. The detection of absence has a certainty level of nearly 100%, since the false detection rate found in the test room is less than one in a million.

5.1.1 Possible interference sources

As mentioned in Section 3.2.2 there has been some problems with air bubbles and bad connectors. Other factors that may prevent or disturb the operation of the system are underfloor heating systems and water pipes in the floor. Concrete reinforcement of the floor has not been found to disturb the system. This is because the reinforcement is usually at a depth of 5 cm or more.

The disturbance caused by underfloor heating systems is unknown. If the conductors of an electric heating system and the water tubes of a hydronic system are installed under a layer of screed, the coexistence of a heating system and the developed system may be possible. However the sensitivity will probably decrease (as impedance decreases) and some 50-Hz mains hum may be present in the signal. If a film-based heating system is

used and there is no screed on top of it, the developed system can not most likely be used. The effect of water pipes in the concrete base of the floor is also unknown.

Water on top the floor causes strong phantom observations, which usually cause a fall alarm. Thus the alarms have to be turned off while the floor is being mopped. However, feedback from the nurses indicates that the detection of moisture on the floor is useful, since urinating on the floor has been known to happen in nursing homes.

Surprisingly electrostatic discharge (ESD) has not caused any problems. The multiplexer design includes resistors connected parallel to each sensor, which discharge static charges. The value for the resistor was chosen so that it is small enough to be effective, but large enough to not to weaken the sensitivity. The value was 6.8 kΩ, which is ten times larger than the typical sensor impedance.

5.2 Person tracking

As presented in publication III, the system that was developed has a positioning accuracy of 21 cm with people who are walking and it can separate two people with a 90% certainty when the gap is 78 cm. The corresponding values for one discrete-signal pressure-sensitive floor sensor are 20 cm and 80 cm [33]. The values are almost identical, even though the system in [33] had four times more sensors per area than the system developed in this work did. This suggests that our analog signals improve the accuracy in relation to sensor resolution. The electric field sensor developed by Valtonen *et al.* tracked walking people with an accuracy of 41 cm [39]. The better accuracy of the system developed here is caused by the smaller sensors. Valtonen *et al.* used sensor elements measuring 60 cm x 60 cm, where our system had sensor dimensions of 36 cm x 30 cm.

The ELSI system can work with ([2], [56], [V]) or without a transponder. This is not possible with the above-mentioned floor sensors. Using *capacitive* RFID tags in random locations, the success rate of identification is relatively poor (93%), the read range is very low (5 mm), and the mean latency is very high (36 s) [V]. These performance values are not acceptable in most cases. The low read range obliges the tag to be placed in a shoe, and because of the high latency and low read range people who are walking cannot be identified. In a fixed location the success rate is high (100%) and the latency is low (0.4 s) [V]. Thus the *capacitive* tag can only be used if the users are instructed to step on marked footprints and stand still until the identification is complete. Using *inductive* RFID tags in random locations, the success rate is 97% and the read range 2.0 m [2]. Because of the higher read range, also moving targets can be identified. Thus only the *inductive* identification method is competitive with other active location systems, which provide identification.

Table 3 presents the performances and key features of the indoor tracking technologies that are available. WLAN tracking is not included, because it operates at the same

frequency band as ZigBee systems and produces similar accuracy. The row labeled ‘Immune to shading’ indicates if walls, furniture, or crowds disturb the signals. Radio frequency systems below a couple of gigahertz (ZigBee, WLAN, RFID, cell phones) can operate through thin interior walls, so they are considered to be immune to shading. However, UWB systems use a bandwidth up to 20 GHz [22], which increases the observed attenuation when the above-mentioned obstructions are present.

Table 3. Comparison of tracking systems.

Technology	NFI	Load-cell	Stereo vision	Ultra-sound	UWB	ZigBee	UHF RFID	Cell phone
Author	Rimminen [III]	Murakita [33]	Harville [25]	Priyanha [21]	Kuhn [22]	Cho [16]	Hähnel [19]	Lakmali [17]
Category	passive or active	passive	passive	active	active	active	active	active
Mean error	21 cm	20 cm	18 cm	10 cm	3 mm	1.8 m	≈ 2 m	8.7 m
Separation at 90% certainty	78 cm	80 cm	N/A	N/A	N/A	N/A	N/A	N/A
Immune to shading	yes	yes	no	no	no	yes	yes	yes
Identifying possible	yes [V], [2], [56]	no	< 2 m [26]	yes	yes	yes	yes	yes
Privacy issues	no	no	yes	no	no	no	no	no
Low computing power	yes	yes	no	yes	yes	yes	yes	yes

5.3 Fall detection

The sensitivity and specificity in fall detection of the system developed in this work is 91% and 91% [IV], and it is immune to shading or changes in the lighting, unlike computer vision. Furthermore, the event set in publication IV included two unclear falls (ending up on one’s knees and ending up sitting), which is not the case with the majority of the related work. The performance of the system developed here with only clear falls included is 96% and 94%. This result is comparable with the majority of the related work.

The key properties and performances of common unobtrusive fall detectors are shown in Table 4. The row labeled ‘Success outside lab’ shows if authors using the particular

technique have data from pilots of field trials to back up their laboratory findings. For example, Alwan *et al.* reported that only false alarms were recorded during their pilot [6], even though the laboratory test indicated perfect performance [45]. In the field trial of Sixsmith and Johnson, too, only one alarm was generated, which was a false one [46]. Field trials of fall detecting with computer vision are scarce.

Table 4. Comparison of unobtrusive fall detectors.

Technology	NFI	Single camera	Single camera	Eight cameras	Vibration sensor	Vibration and PIR	IR
Author	Rimminen [IV]	Lee [51]	Foroughi [50]	Auvinet [52]	Alwan [45]	Toreyin [47]	Sixsmith [46]
Sensitivity	90.7% (95.6%)	77%	92.8%	100%	100%	100%	36.7%
Specificity	90.6% (94.2%)	95%	97.6%	100%	100%	100%	100%
Success outside lab	yes [77]	not found	not found	not found	no [6]	not found	no [46]
Sample size	650	315	1250	28	123	163	not clear
Number of subjects	10	21	50	1	2 dummies	not clear	1
Number of event types	17	5	10	14	9	4	30
Low computing power	yes	no	no	no	yes	yes	yes
Detects low-impact falls	yes	yes	yes	yes	no	yes	yes
Privacy issues	no	yes	yes	yes	no	no	no
Immune to shading	yes	no	no	no	yes	no	no

The performance of ELSI without unclear falls is in parentheses.

The problem with most fall detectors is that they have not been tested in everyday practice [13]. In 2009 Oksanen *et al.* reported that the system developed in this work works well in building ‘G’ at Kustaankartano [77]. In that study fall detection was also tested by the nurses in 16 patient rooms, yielding a sensitivity and specificity of 79% and 100%. Though it had an intentionally different bias, the result matches the one in publication IV. This suggests that the method is feasible for use in nursing homes.

Pre-fall behavior, such as stumbling or staggering, cannot currently be detected with the system developed here. Accelerometers worn by the subject may make this possible. However, walking along walls could reveal the deterioration of balance and could be detected with the system that was developed. Furthermore, the majority of falls among the in-patient elderly happen immediately after getting out bed or in a toilet [10]. This information is available using the system developed here and could be used for sending a fall warning signal if the person is known to have a high risk of falling.

The prevention of falls could be possible if the system developed here was used to control the lighting. The system could switch on the lights when a person gets out of bed during the night. There is some correlation between poor lighting and falls among senior citizens, as it is the fourth most significant factor in a principal components analysis carried out by Northridge *et al*. [78]. The study group consisted of people between ages of 60-93, who had fallen at least once during the previous year. However, special attention will be needed, since bright lights after a rest period may actually increase the risk of falling. The use of dim lights has been suggested to solve this problem [79]. Thus the lights should be dim when switched on during the night.

5.4 Biosignals

The effect of posture and the measurement point was determined by using five test subjects. In the prone position, heart activity is visible at chest height and at abdominal height. In the supine position, only abdominal height produced a clear signal. Other postures produce weak signals. Respiratory activity is visible in prone and supine postures when measured at abdominal height. It is evident that the measurement should be taken from abdominal height.

As far as we know, there are no passive systems available, which combine tracking, fall detection and vital function monitoring. Active systems enable this combination [80], however the disadvantages of active systems have been discussed earlier.

5.5 User experiences

5.5.1 Nursing home staff

The staff of Kustaankartano's building 'G' has put the system into everyday use and their attitude towards it can be described as positive. In a study by Oksanen *et al.*, the opinions of thirty nurses that had used the system for one year were gathered using a Quebec user evaluation of satisfaction with assistive technology (QUEST) 2.0 query. They gave the whole system a mean grade of 4/5 and the score for the sensor floor itself was also 4/5 [77].

They comment that the system makes their work more effective, especially at night-time [81]. The system can be configured to produce the following alarms: falling, getting out of bed, entering the toilet, entering the room, and exiting from the room. The fall alarms, bed-exiting alarms, and toilet-entering alarms have been found useful. The nurses have reported that the bed exit alarm is especially useful during the night shift. The system still gives some false positive alarms, but this has been a known selection [82].

The first large-scale installation of the ELSI system in building 'G' of Kustaankartano may be considered a success. At the time of writing it was announced that building 'D' (identical to building 'G') is facing a full renovation in 2011, and two floors may be equipped with the ELSI system [83].

5.5.2 The users under monitoring

One senior citizen and his family members have indicated their satisfaction with the system. A newspaper article discusses the 77-year-old man living independently and successfully using the system in the Harjula Settlement Association [84]. After having had a stroke, he has become careful and is aware of the dangers of living alone. The system has been configured to generate alarms of falls and of long periods of inactivity, which are sent to the cell phones of his children. The system has increased the feeling of safety of both him and his children. This indicates that the system has had a positive effect on his life.

Feedback from residents in the Kustaankartano center for the elderly is not available, because the residents using the system that are in long-term care suffer from dementia. The ones that have no mental impairments are in short-term care and are just passing by, having no time to get familiar with the system. As mentioned in the introduction, the system is intended to prolong independent living. During the work on this thesis no proof of this has yet been obtained.

5.6 Ongoing and future studies

The potential of the proposed technology is not limited to the aforementioned applications. We are planning on study if the monitoring of the long-term activity and the statistical analysis of behavioral patterns could be used for determining and tracking the overall health status of a senior citizen [81]. In other application fields we aim to determine if the vital function measurement could be used in seclusion monitoring of the intoxicated. The system has been installed in one seclusion room in the Lohja hospital [81], and may be possibly installed in two lock-up rooms of the police in Hämeenlinna. The vital function measurement could also be used to determine if a fall alarm has been caused by a real person or by some form of disturbance. The system could also be used for building automation and interactive environments [85], and it could provide rehabilitation services for stroke patients [86].

6 Conclusions

It has been found that remote monitoring relieves the stress inflicted on the caregivers in care for the elderly. The monitoring may also increase the senior citizens' feeling of safety and their perceived quality of life. [6] It is also known that call systems do not work as well as expected when falls among the elderly are studied [12]. Automatic fall detectors worn by the user could solve this, but such devices are sometimes removed by people suffering from dementia [18]. Since the ELSI system is capable of remote monitoring and generating alarms without user input and without devices to be worn, its advantages are clear in care for the elderly.

The goals of this thesis were generally reached well. The main conclusions and how each of the goals was reached are summarized below.

1.1) A good sensitivity was achieved, and the system works regardless of the type of footwear.

1.2) The accuracy and discrimination performance are considered to be more than adequate for the purposes of care for the elderly and for context-aware computing. The accuracy is competitive with other floor sensors and with transponder-based tracking systems.

1.3) The scalability of the ELSI system is good, since the system can be used to cover rooms with various shapes and sizes and it can cover a single room or the entire building. The system is also undetectable and discreet.

1.4) Water on the floor, air bubbles beneath the flooring and oxidation in the sensor connectors may cause false observations.

2.1) The fall detection performance is considered to be good, as it is competitive with single-camera computer vision.

2.2) Entering and leaving the area being monitored can be detected with good certainty. This enables detection of exiting from the room and getting out of bed.

3.1) Posture has a significant effect on the quality of the biosignal recorded from a person lying on the floor. Thus it is concluded that the system developed here cannot be used in the monitoring of critical vital functions and should only be used to provide additional information.

3.2) The system can be used without tags, but if the identification of people is required, RFID tags can be used. The use of *capacitive* tags is feasible if the

users are instructed to step on marked footprints and stand still until the identification is complete.

3.3) When *inductive* RFID tags are used, also moving targets can be identified. This creates a robust platform for truly context-aware computing.

4.1) Feedback from nurses in a large nursing home indicates that they are satisfied with the system. The result is based on a questionnaire with thirty participants that had used the system for one year.

4.2) Feedback from one independently living senior citizen indicates that he and his family members are generally happy with the system.

References

[1] H. Rimminen, "Kapasitiivisen anturin elektroniikka," Master's thesis, Department of Electrical and Communications Engineering, Helsinki University of Technology, Apr. 2006. (in Finnish)

[2] A. Ropponen, H. Rimminen, and R. Sepponen, "Robust system for indoor localization and identification," *Wireless Personal Communications*. (in press)

[3] A. Romppanen, "On the labour market effects of ageing," *Publications of Ministry of Social Affairs and Health*, Helsinki, 2000. (in Finnish)

[4] P. Parkkinen, "Väestön ikääntymisen vaikutukset kunnantalouteen," *Research reports 136, Government Institute for Economic Research*, Helsinki, Dec. 2007. (in Finnish)

[5] B. G. Celler, W. Earnshaw, E. D. Ilsar, L. Betbeder-Matibet, M. F. Harris, R. Clark, T. Hesketh, and N. H. Lovell, "Remote monitoring of health status of the elderly at home. A multidisciplinary project on aging at the University of New South Wales," *International Journal of Bio-Medical Computing*, vol. 40, no. 2, pp. 147-155, Oct. 1995.

[6] C. Swedberg, "Wright university researchers test RFID and ultrasound for 3-D RTLS," *RFID Journal*, 20 Apr. 2010 [Online]. Available: http://www.rfidjournal.com/article/print/7546

[7] M. Alwan, D. C. Mack, S. Dalal, S. Kell, B. Turner, and R. A. Felder, "Impact of passive in-home health status monitoring technology in home health: Outcome pilot," in *Proc. 1st Transdisciplinary Conference on Distributed Diagnosis and Home Healthcare*, Arlington, VA, US, 2006, pp. 79-82.

[8] T. Hori, Y. Nishida, H. Aizawa, S. Murakami, and H. Mizoguchi, "Sensor network for supporting elderly care home," in *Proc. Third IEEE International Conference on Sensors*, vol. 2, Vienna, Austria, 2004, pp. 575-578.

[9] M. Motoki, I. Sadanori, and K.Susumu, "An empirical study of an RFID mat sensor system in a group home," *Journal of Networks*, vol. 4, no. 2, 2009, pp. 133-139.

[10] C. Vass, O. Sahota, A. Drummond, D. Kendrick, J. Gladman, T. Sach, M. Avis, and M. Grainge, "REFINE (Reducing Falls in In-patient Elderly) - a randomised controlled trial," *Trials journal*, vol. 10, no. 83, Sep. 2009.

[11] M. E. Tinetti, M. Speechley, and S. F. Ginter, "Risk factors for falls among elderly persons living in the community," *The New England Journal of Medicine*, vol. 319, no. 26, pp. 1701-1707, Dec. 1988.

[12] J. Fleming and C. Brayne, "Inability to get up after falling, subsequent time on floor, and summoning help: prospective cohort study in people over 90," *Biomedical Journal*, no. 337, article no. 2227, pp. 1279-1282, Nov. 2008.

[13] J. Campbell, "Falls in older people," *Biomedical Journal*, no. 337, article no. 2320, pp. 1247-1248, Nov. 2008.

[14] J. Hightower and G. Borriello, "A survey and taxonomy of location systems for ubiquitous computing," *IEEE Computer*, vol. 34, no. 8, pp. 57-66, Aug. 2001.

[15] P. Hii and A. Zaslavsky, "Improving location accuracy by combining WLAN positioning and sensor technology," in *Workshop on Real-World Wireless Sensor Networks*, Stockholm, Sweden, 2005.

[16] H. Cho, M. Kang, J. Park, B. Park, and H. Kim, "Performance analysis of location estimation algorithm in ZigBee networks using received signal strength," in *Proc. 21st International Conference on Advanced Information Networking and Applications Workshops*, Niagara Falls, Canada, 2007, pp. 302-306.

[17] B. D. S. Lakmali and D. Dias, "Database correlation for GSM location in outdoor & indoor environments," in *Proc. 4th International Conference on Information and Automation for Sustainability*, Colombo, Sri Lanka, 2008, pp. 42-47.

[18] C. C. Lin, P. Y. Lin, P. K. Lu, G. Y. Hsieh, W. L. Lee, and R. G. Lee, "A healthcare integration system for disease assessment and safety monitoring of dementia patients," *IEEE Transactions on Information Technology on Biomedicine*, vol. 12, no. 5, pp. 579-586, Sept. 2008.

[19] D. Hähnel, W. Burgard, D. Fox, K. Fishkin, and M. Philipose, "Mapping and localization with RFID technology," in Proc. *the IEEE International Conference on Robotics & Automation*, New Orleans, LA, 2004, pp. 1015-1020.

[20] S. Willis and S. Helal, "RFID information grid and wearable computing solution to the problem of wayfinding for the blind user in a campus environment," in *Proc. Ninth IEEE International Symposium on Wearable Computers*, Osaka, Japan, 2005, pp. 1-8.

[21] N. B. Priyantha, "The Cricket indoor location system," Doctoral thesis, Department of Computer Science, Massachusetts Institute of Technology, Jun. 2005.

[22] M. Kuhn, Z. Cemin, B. Merkl, Y. Depeng, W. Yazhou, M. Mahfouz, and A. Fathy, "High accuracy UWB localization in dense indoor environments," in *Proc. The IEEE International Conference on Ultra-Wideband*, vol. 2, Hannover, Germany, 2008, pp. 129-132.

[23] A. Kaushik, N. Lovell, and B. Celler, "Evaluation of PIR detector characteristics for monitoring occupancy patterns of elderly people living alone at home," in *Proc. 29th Annual International Conference of the IEEE Engineering in Medicine and Biology Society*, Lyon, France, 2007, pp. 3802-3805.

[24] R. Want, A. Hopper, V. Falcão, and J. Gibbons, "The Active Badge location system," *ACM Transactions on Information Systems*, vol. 10, no. 1, pp. 91-102, Jan. 1992.

[25] M. Harville, “Stereo person tracking with adaptive plan-view templates of height and occupancy statistics,” *Image and Vision Computing, Statistical Methods in Video Processing*, vol. 22, no. 2, pp. 127-142, Feb. 2004.

[26] D. López de Ipiña, P. Mendonça, and A. Hopper, “TRIP: A low-cost vision-based location system for ubiquitous computing,” *Personal Ubiquitous Computing*, vol. 6, no. 3, pp. 206-219, May 2002.

[27] M. Williams, “Better face-recognition software,” *Technology Review*, 30 May, 2007 [Online]. Available: http://www.technologyreview.com/infotech/18796/?a=f

[28] C. BenAbdelkader, R. Cutler, and L. Davis, “Stride and cadence as a biometric in automatic person identification and verification,” in *Proc. Fifth IEEE International Conference on Automatic Face and Gesture Recognition*, Washington, DC, 2002, pp. 372-377.

[29] M. D. Addlesee, A. Jones, F. Livesey, and F. Samaria, “The ORL active floor,” *IEEE Personal Communications*, vol. 5, no. 4, pp. 35-41, Oct. 1997.

[30] R. J. Orr and G. D. Abowd, “The smart floor: a mechanism for natural user identification and tracking,” in *Proc. Conference on Human Factors in Computing Systems*, The Hague, The Netherlands, 2000, pp. 275-276.

[31] Y. Kaddoura, J. King, and A. Helal, “Cost-precision tradeoffs in unencumbered floor-based indoor location tracking,” in *Proc. Third International Conference On Smart Homes and Health Telematic*, Québec, Canada, 2005, pp. 75-82.

[32] W. H. Liau, C. L. Wu, and L. C. Fu, “Inhabitants tracking system in a cluttered home environment via floor load sensors,” *IEEE Transactions on Automation Science and Engineering*, vol. 5, no. 1, pp. 10-20, Jan. 2008.

[33] T. Murakita, T. Ikeda, and H. Ishiguro, “Human tracking using floor sensors based on the Markov chain Monte Carlo method,” in *Proc. 17th International Conference on Pattern Recognition*, vol. 4, Cambridge, UK, 2004, pp. 917-920.

[34] M. Paajanen, J. Lekkala, and K. Kirjavainen, “Electromechanical film (EMFi) - A new multipurpose electret material,” *Sensors and Actuators A: Physical*, vol. 84, no. 1-2, pp. 95-102, Aug. 2000.

[35] M. Eyole-Monono, R. Harle, and A. Hopper, “POISE: An inexpensive, low-power location sensor based on electrostatics,” In *Proc. 3rd Annual International Conference On Mobile and Ubiquitous Systems: Networks And Services*, San Jose, CA, 2006, pp. 1-3.

[36] J. Suutala, S. Pirttikangas, J. Riekki, and J. Röning, “Reject-optional LVQ-based two-level classifier to improve reliability in footstep identification,” in *Proc. Second International Conference on Pervasive Computing*, Vienna, Austria, 2004, pp. 182-187.

[37] T. G. Zimmerman, J. R. Smith, J. A. Paradiso, D. Allport, and N. Gershenfeld, “Applying electric field sensing to human-computer interfaces,” in *Proc. SIGCHI*

Conference on Human Factors in Computing Systems, Denver, CO, 1995, pp. 280-287.

[38] D. Savio and T. Ludwig, "Smart carpet: a footstep tracking interface," In *Proc. 21st International Conference on Advanced Information Networking and Applications Workshops*, Niagara Falls, Canada, 2007, pp. 754-760.

[39] M. Valtonen, J. Mäentausta, and J. Vanhala, "TileTrack: capacitive human tracking using floor tiles," in *Proc. IEEE International Conference on Pervasive Computing and Communications*, Galveston, TX, 2009, pp. 1-10.

[40] N. Noury, A. Fleury, P. Rumeau, A. K. Bourke, G. Ó. Laighin, V. Rialle, and J. E. Lundy, "Fall detection – Principles and methods," in *Proc. 29th Annual International Conference of the IEEE Engineering in Medicine and Biology Society*, Lyon, France, 2007, pp. 1663-1666.

[41] A. K. Bourke, V. J. O'Brien, and G. M. Lyons, "Evaluation of a threshold-based tri-axial accelerometer fall detection algorithm," *Gait & Posture*, vol. 26, no. 2, pp. 194-199, Sep. 2006.

[42] M. Kangas, I. Vikman, J. Wiklander, P. Lindgren, L. Nyberg, and T. Jamsa, "Sensitivity and specificity of fall detection in people aged 40 years and over," Gait & Posture, vol. 29, no. 4, pp. 571-574, Jun. 2009.

[43] A. K. Bourke and G. M. Lyons, "A threshold-based detection algorithm using a bi-axial gyroscope sensor," *Medical Engineering & Physics*, vol. 30, no. 1, pp. 84–90, Jan. 2007.

[44] G. Wu and S. Xue, "Portable preimpact fall detector with inertial sensors," *IEEE Transactions on Neural Systems and Rehabilitation Engineering*, vol. 16, no. 2, pp. 178-183, Apr. 2008.

[45] M. Alwan, P. J. Rajendran, S. Kell, D. Mack, S. Dalal, M. Wolfe, and R. Felder, "A smart and passive floor-vibration based fall detector for elderly," in *Proc. 2nd International Conference on Information and Communication Technologies*, Damascus, Syria, 2006, pp. 1003-1007.

[46] A. Sixsmith and N. Johnson, "A smart sensor to detect the falls of the elderly," *IEEE Pervasive Computing*, vol. 3, no. 2, pp. 42-47, Apr. 2004.

[47] B. Toreyin, E. Soyer, Onaran, and A. Cetin, "Falling person detection using multisensor signal processing," *EURASIP Journal on Advances in Signal Processing*, vol. 2008, article no. 29, pp. 1-7, Jan. 2008.

[48] D. Anderson, J. Keller, M. Skubic, X. Chen, and Z. He, "Recognizing falls from silhouettes," in *Proc. 28th Annual International Conference of the IEEE Engineering in Medicine and Biology Society*, New York, NY, 2006, pp. 6388-6391.

[49] B. Huang, G. Tian, and H. Wu, "A method for fast fall detection based on intelligent space," in *Proc. IEEE International Conference on Automation and Logistics*, Qingdao, China, 2008, pp. 2260-2265.

[50] H. Foroughi, B. S. Aski, and H. Pourreza, “Intelligent video surveillance for monitoring fall detection of elderly in home environments,” in *Proc. 11th International Conference on Computer and Information Technology*, Khulna, Bangladesh, 2008, pp. 219-224.

[51] T. Lee and T. A. Mihailidis, “An intelligent emergency response system: preliminary development and testing of automated fall detection,” *Journal of Telemedicine and Telecare*, vol. 11, no. 4, pp. 194-198, Jun. 2005.

[52] E. Auvinet, L. Reveret, A. St-Arnaud, J. Rousseau, and J. Meunier, “Fall detection using multiple cameras,” in *Proc. 30th Annual International Conference of the IEEE Engineering in Medicine and Biology Society*, Vancouver, Canada, 2008, pp. 2554-2557.

[53] C. J. Harland, T. D. Clark, and R. J. Prance, “Electric potential probes — New directions in the remote sensing of the human body,” *Measurement Science and Technology*, vol. 13, no. 2, pp. 163-169, Dec. 2001.

[54] W. J. Smith and J. R. LaCourse, “Non-contact biopotential measurement from the human body using a low-impedance charge amplifier,” in *Proc. IEEE 30th Annual Northeast Bioengineering Conference*, Springfield, MA, 2004, pp. 31-32.

[55] J. Alametsä, A. Värri, M. Koivuluoma, and L. Barna, ”The potential of EMFi sensors in heart activity monitoring,” in *Proc. 2nd OpenECG Workshop on Integration of the ECG into the EHR & Interoperability of ECG Device Systems*, Berlin, Germany, 2004, pp. 1-5.

[56] A. Ropponen, M. Linnavuo and R. Sepponen, “LF indoor location and identification system,” *International Journal on Smart Sensing and Intelligent Systems*, vol. 2, no. 1, pp. 94-117, Mar. 2009.

[57] T. G. Zimmerman. “Personal area networks: near-field intrabody communication,” *IBM Systems Journal*, vol. 35, no. 3&4, pp. 609-617, 1996.

[58] I. L. Al-Qadi, O. A. Hazim, W. Su, and S. M. Riad, “Dielectric properties of Portland cement concrete at low radio frequencies,” *Journal of Materials in Civil Engineering*, vol. 7, no. 3, pp. 192-198, Aug. 1995.

[59] S. Gabriel, R. W. Lau, and C. Gabrie, “The dielectric properties of biological tissues: II. Measurements in the frequency range 10 Hz to 20 GHz,” *Physics in Medicine and Biology*, vol. 41, no. 11, pp. 2251-2269, Nov. 1996.

[60] R. Matthes, “Guidelines for limiting exposure to time-varying electric, magnetic, and electromagnetic fields (Up to 300 GHz),” *Health Physics*, ICNIRP Guidelines, vol. 74, no. 4, p. 509, Apr. 1998.

[61] M. Bramanti, “A high sensitivity measuring technique for capacitive sensor transducers,” *IEEE Transactions on Industrial Electronics*, vol. 37, no. 6, pp. 584-586, Dec. 1990.

[62] Agilent Technologies, Inc., *Impedance Measurement Handbook - A guide to measurement technology and techniques* (4th ed.), Application note, Santa Clara, CA: 2009, pp. 2-2 – 2-3.

[63] Texas Instruments Inc., "LM555, NE555, SA555, SE555 Precision Timers," Datasheet, Sep. 1973, Rev. G, Jun. 2008.

[64] G. J. Yeh, I. Dendo, and W. H. Ko, "Switched-capacitor interface circuit for capacitive transducers," in *Proc. International Conference on Solid-State Sensors and Actuators*, Philadelphia, PA, 1985, pp. 60-63.

[65] W. Ahmad, "A new simple technique for capacitance measurement," *IEEE Transactions on Instrumentation and Measurement*, vol. 35, pp. 640-641, Dec. 1986.

[66] S. S. Awad, "Capacitance measurement based on an operational amplifier circuit: Error determination and reduction," *IEEE Transactions on Instrumentation and Measurement*, vol. 37, no. 3, pp. 379-382, Sep. 1988.

[67] M. Brychta, "Measure capacitive sensors with a sigma-delta modulator," *Electronics Design*, Apr. 28, 2005 [Online]. Available: http://electronicdesign.com/article/analog-and-mixed-signal/measure-capacitive-sensors-with-a-sigma-delta-modu.aspx

[68] A. S. Sedra and K. C. Smith, *Microelectronic circuits*, 4th ed. Oxford, NY: Oxford University Press, 1998, pp. 73-78, 86-88, 936-937.

[69] K. Silvonen, *Sähkötekniikka ja Elektroniikka*, Helsinki, Finland: University Press Finland, 2003, pp. 194. (in Finnish)

[70] P. Horowitz and W. Hill, *The Art of Electronics*, 2nd ed. Cambridge, UK: Cambridge University Press, 1994, pp.1031-1033.

[71] National Semiconductor Corp., "High Q notch filter," *Linear Brief series*, no. 5, Mar. 1969.

[72] D. K. Barton, *Radar System Analysis and Modeling*. Norwood, MA: Artech House, 2005, p. 45.

[73] R. E. Kalman, "A new approach to linear filtering and prediction problem," *Transactions of the ASME – Journal of Basic Engineering*, no. 82, series D, pp. 35-45, 1960.

[74] M. S. Arulampalam, S. Maskell, N. Gordon, and T. Clapp, "A tutorial on particle filters for online nonlinear/non-Gaussian Bayesian tracking," *IEEE Transactions on Signal Processing*, vol. 50, no.2, pp.174-188, Feb. 2002.

[75] S. Särkkä, A. Vehtari, and J. Lampinen, "Rao-Blackwellized Monte Carlo data association for multiple target tracking," in *Proc. Seventh International Conference on Information Fusion*, Stockholm, Sweden, 2004, pp. 583-590.

[76] J. Diard, P. Bessiere, and E. Mazer, "A survey of probabilistic models using the Bayesian programming methodology as a unifying framework," in *Proc. 2nd*

International Conference on Computational Intelligence, Robotics and Autonomous Systems, Singapore, 2003, pp. 1-8.

[77] R. Oksanen, S. Paldanius, J. Nykänen, M. Linnavuo, K. Raivio, E. Segerholm, R. Sepponen, L. Pohjola, and H. Finne-Soveri, "Testing and adopting floor-sensor solutions in daily practice for patient safety in Kustaankartano nursing home," Abstract in *Journal of Nutrition Health and Aging*, vol. 13, supplement 1, pp. S361, Jul. 2009 and Poster in *19th IAGG World Congress of Gerontology and Geriatrics*, Paris, France, 2009. [Online]. Available: http://www.hel.fi/wps/wcm/connect/a3b1c9004288a2779b349b7eec66b6f2/3_innokusti_astu.pdf?MOD=AJPERES

[78] M. E. Northridge, M. C. Nevitt, J. L. Kelsey, and B. Link, "Home Hazards and Falls in the Elderly: The Role of Health and Functional Status," *American Journal of Public Health*, vol. 85, no. 4, pp. 509-515, Apr. 1995.

[79] A. Gabell, M. A. Simons, and U. S. L. Nayak, "Falls in the healthy elderly: predisposing causes," *Ergonomics*, vol. 28, no. 7, pp. 965-975, Jul. 1985.

[80] J. M. Kang, T. Yoo, H. C. Kim, "A Wrist-Worn Integrated Health Monitoring Instrument with a Tele-Reporting Device for Telemedicine and Telecare," *IEEE Transactions on Instrumentation and Measurement*, vol. 55, no. 5, pp.1655-1661, Oct. 2006.

[81] M. Linnavuo and H. Rimminen, "Localization and monitoring of people with a near-field imaging system – boosting the elderly care," in *Pervasive and smart technologies for healthcare: ubiquitous methodologies and tools*, A. Coronato and G. De Pietro, Eds. Hershey, NY: IGI Global, 2010, pp. 78-96, ch. 4.

[82] O. Skogberg, "Golvet vet när någon rör sig," *Huvudstadsbladet*, Jul. 26, 2009, p. 4. (in Swedish)

[83] "Kustaankartanoon lisää remontteja," *Helsingin uutiset, Lyhyet*, Apr. 8-9, 2010. (in Finnish)

[84] S. Palokari, "Turvana hälyttävä matto," *Helsingin sanomat*, Nov. 5, 2007, p. D4. (in Finnish)

[85] J. Teirikangas, S. Uotinen, J. Kuutti, J. Jokelainen, H. Tuoma, and A. Kivilahti, "Anturiverkko mittaa väenkulkua," *Prosessori*, May 2010, pp. 20-23. (in Finnish)

[86] M. Linnavuo, A. Ojapelto, and R. Sepponen, "A proactive space for rehabilitation, gaming and multimodal interaction," poster at *Proc. 13th International MindTrek Conference: Everyday Life in the Ubiquitous Era*, Tampere, Finland, 2009, p. 213.

ISBN 978-952-60-3496-6 (paper)
ISBN 978-952-60-3497-3 (electronic)
ISSN 1456-1174 (paper)
ISSN 1459-1111 (electronic)
Multiprint Oy
Espoo 2011